THERMAL AND THERMOHYDRAULIC EFFICIENCY ENHANCEMENT OF A DOUBLE PASS SOLAR AIR HEATER USING DISCRETE RIBS ON ABSORBER PLATE

DISSERTATION

Submitted in Partial Fulfillment of the
Requirement for Award of the Degree of

MASTER OF TECHNOLOGY

in

MECHANICAL ENGINEERING

By

DINKAR PRASAD SINGH
(Reg. No. 11001320)

Under the Guidance of
Mr. SUDHANSHU DOGRA
(Assistant Professor)

DEPARTMENT OF MECHANICAL ENGINEERING

LOVELY PROFESSIONAL UNIVERSITY

PHAGWARA, PUNJAB (INDIA) -144402

(MAY-2015)

Lovely Professional University, Phagwara, Punjab

CERTIFICATE

I hereby certify that the work which is being presented in the thesis entitled **"Thermal and Thermohydraulic Efficiency Enhancement of a Double Pass Solar Air Heater Using Discrete Ribs on Absorber Plate"** in partial fulfillment of the requirement for the award of degree of **Master of Technology** and submitted in Department of Mechanical Engineering, Lovely Professional University, Phagwara, Punjab, is an authentic record of my own work carried out during period from January 2014 to May 2015 under the supervision of Mr. Sudhanshu Dogra**,** Assistant Professor, Department of Mechanical Engineering, Lovely Professional University, Phagwara, Punjab.

The matter presented in this dissertation has not been submitted by me anywhere for the award of any other degree or to any other institute. .

Date: …../…../…….. **(Dinkar Prasad Singh)**

This is to certify that the above statement made by the candidate is correct to best of my knowledge.

Date: …../…../……. **(Mr. Sudhanshu Dogra)**
Supervisor

The M. Tech Viva- Voce examination of Dinkar Prasad Singh, has been held on …./…./……

Signature of Examiner

Signature of External Examiner

ACKNOWLEDGEMENT

I take this opportunity to place on record of my profound sense of indebtedness and deep appreciation to my supervising guide, ***Mr. Sudhanshu Dogra, Assistant Professor****, Department of Mechanical Engineering, Lovely Professional University, Phagwara, Punjab, for his personnel encouragement, unending benevolence, parentally behavior, stimulating discussion and guiding from the beginning to the date of the fruition of this thesis, my gratitude to him no bounds.*

I deeply indebted to Mr. Nitin Chauhan, Assistant Professor and Mr. Sandeep Singh, Assistant Professor, Department of Mechanical Engineering for all the assistance that they extended to me during my research work. They were always a source of encouragement and showed keen interest in my progress

I would like to express deep appreciation to Mr. Raj Shekhar Dondapati, Research Coordinator and Assistant Professor, Department of Mechanical Engineering, who always assisted me during studies and progress of my work.

I am extremely thankful to Mr. Gurpreet Singh Phull, Deputy Dean of Mechanical Engineer and Dr. Rajeev Kumar, Head of Department of Mechanical Engineer, Lovely Professional University for his support, encouragement throughout the work and all the facilities extended to me in the department.

I would like to express my sincere thanks to all the faculty member of Department of Mechanical Engineering, Lovely Professional University, Phagwara, Punjab and the non-teaching staff for their timely help and co-operation.

Whatever I write here will be ineffable to express my sense of indebtedness to my father and mother; and finally I am thankful to the grace of almighty god who let me dedicate this work to my adored parents and all my dear friends.

- Dinkar Prasad Singh

ABSTRACT

Solar energy is the most important renewable energy resource due to its easy availability and abundance. For the purpose of minimizing the energy loss and to maximize the utilization of solar energy for low grade thermal applications, absorbent materials have been effectively employed as energy captivating medium. Solar air heaters are easily fabricated with cheaper material as compared to solar water heaters. It produces hot air for industrial applications as drying the food, space heating etc. Thermal efficiency of solar air heater is poor due to its low rate of heat transfer. For increasing the efficiency of heat transfer, artificial roughness in the form of ribs is created over the absorber plate which tends to increase the turbulence of air, thereby increasing the vortex flow over the plate. By experimenting the effect of different ribs geometry over the absorber plate, enhancement of Nusselt number and friction factor is calculated and apart from this some correlations were also developed on account of the values coming from the experiment.

This thesis presents the effect of heat transfer and friction factor of discrete ribs on the both side of absorber plate in double pass solar air heater. These effects depends upon the relative roughness height of (e/D_h) 0.044, the relative roughness pitch (p/e) of 5, 10 and 20 and angle of attack (α) of 30°, 60˚and 90˚. Reynold number varies from 6900-14000. The aspect ratio (W/H) of experimental setup is 10. The maximum heat transfer and friction factor is observed at relative roughness pitch (p/e) of 10 and angle of attack (α) of 60˚. Also the maximum value of thermal and thermohydraulic efficiency is observed at same relative roughness pitch of 10 and angle of attack (α) 60˚. It also shows that the performance of double pass solar air heater is higher than the single pass air heater.

TABLE OF CONTENTS

LIST OF TABLES

LIST OF FIGURES

NOMENCLATURE

A_C	Area of absorber plate (m^2)
A_0	Throat area of orifice meter (m^2)
ASHARE	American Society of Heating, Refrigerating, and Air Condensing Engineers
BTU	British Thermal unit
C_P	Specific heat (J/Kg K)
C_d	Coefficient of discharge of orifice meter
D	Effective diameter
D_h	Hydraulic diameter (m)
d/W	Relative gap position
e	Roughness element height (mm)
e/D_h	Relative roughness element
f	Friction factor
f_S	Friction factor for smooth plate
g/e	Relative gap width
h	Heat transfer coefficient (W/m^2K)
k	Thermal conductivity(W/m K)
l/s	Relative grit length
m	Mass flow rate (Kg/s)
Nu	Nusselt number

Nu_s	Nusselt number for smooth plate
p	Pitch (m)
p/e	Relative roughness pitch
Q_u	Heat gain (Watt)
Re	Reynold number
Tf	Bulk mean air temperature (°C)
Tp	Average plate temperature (°C)
W/H	Aspect ratio
A	Angle of attack (α)
β	Ratio between orifice diameter to pipe diameter
ΔP_o	Pressure drop across orifice meter (N/m^2)
ρ	Density of air (Kg/m^3)
φ	Chamfer angle

CHAPTER 1 INTRODUCTION

1.1 INTRODUCTION

Energy is an important input for economic development and improving quality of life as it is a key factor in defining the commercial development of all countries. India's per capita ingestion of commercial energy (e. g. coal, petroleum and electricity) is only 1/8th of global average and will increase with growth in GDP and perfection in standard of living. Comm – ercial energy is used in the country half of the total energy and the rest imminent from non commercial resources like cow dung, fuel wood and wastage of agriculture [1]. In an effort to meet the demands of a developing nation, the Indian energy sector has witnessed a rapid growth. Areas like the resource exploration and exploitation, capacity additions, and energy sector reforms have been revolutionized. Everything happens in this world is expression of the flow of energy forms. The percentage use of various sources of energy consumed by the world is given in Table 1 [2].

Table. 1 Percentage use of sources consumed by world [2]

Energy Sources	**Oil**	**Coal**	**Gas**	**Uranium**	**Hydro**	**Dung**	**Waste**	**Wood**
Utilization	38.3%	32.5%	19%	0.13%	2.0%	1.2%	0.3%	6%

Oil, coal, gas, uranium and hydro which are about 92% are commonly known as commercial or conventional energy sources. Non- commercial sources like firewood, animal dung and agriculture waste represent 8 % of total energy used in the world [2].

Classifications of energy sources into three ways:

i) Primary Energy Sources: Primary energy sources can be defined as sources which provide a net supply of energy. Coal, Oil, Uranium etc. are some of the examples of this type. The energy required to obtain these fuels is much less than the energy produced during combustion with very high energy yield ratio. The primary fuels only can accelerate growth but their supply is limited.

ii) Secondary Energy Sources: They produce no net energy and their yield is less than the input. Example is intensive agriculture, solar energy, Wind energy, Water energy, Tidal energy etc.

iii) Supplementary Energy Sources: These are those energy sources whose net energy yield is zero. They require highest investment in terms of energy. Thermal insulation is an example of this type [2].

If the present trend continues, the world will be very crowded in the coming years. The world population may reach 10 billion in the recent years. The conventional energy sources like coal, wood, petrol etc. are reducing very fast whereas nuclear energy requires a lot of experts and safety against nuclear radiations. Also these are not good for health as they produce a lot of pollution and damage to our body. So there is a need of switching over to non-conventional energy source like solar energy, wind energy, tidal energy etc. which are non-exhaustible types of energy sources and produce no pollution. Today every country draws its energy requirements from a variety of sources and uses them in different areas.

1.2 SOLAR ENERGY

The sun is the prominent source of the energy we use on earth. Solar energy is very large, inexhaustible source of energy. The power from the sun intercepted by the earth is approximately 1.8×10^{11} MW, which is thousands of times larger than the present consumption rate on the earth of all commercial energy sources. Thus solar energy could supply all the present and future energy needs of the world on a continuing basis. This makes it one of the most promising unconventional energy sources [1, 3].

Sun is the source of many forms of energy accessible to us. Hydrogen is the most abundant element at high temperature, high pressure and high density undergoes nuclear fusion and hence releases an enormous amount of energy. The energy received from the sun on a unit area perpendicular to the direction of propagation of radiation outside atmosphere is called solar constant, and has a value 1353 W/m2 . The energy received from the sun on a unit area perpendicular to the direction of propagation of radiation outside atmosphere is called solar constant, and has a value 1353 W/m^2 and when received on the earth has a value of 1100 W/m^2 and is variable. This energy is typically converted into usual energy form through natural and man- made processes [1].

The applications of solar energy which are enjoying most success today are [3]:

(1) Heating and cooling of housing building.
(2) Solar water heater
(3) Solar dryer for agriculture.
(4) Solar distillation System.
(5) Salt production by evaporation of sea water or in land brines.

1.3 SOLAR COLLECTOR

Solar collectors are the collection devices which increase the flux on the absorber surface as compared to the flux impacting on the concentrator surface. Due to the apparent motion of the Sun, the concentrating surface, whether reflecting or refracting will not be in a position to redirect the sun rays onto the absorber, throughout the day if both the concentrator surface and absorber are stationary. The solar energy thus collected is carried from the circulating fluid either directly to the hot water or space conditioning equipment or to a thermal energy storage tank from which can be drawn for use at night or cloudy days [4]. The utilization of solar energy requires solar collectors. There are general two types:

1. Non-concentrating or stationary
2. Concentrating

1.3.1. Non-Concentrating or Stationary Collectors

These collectors are permanently fixed in position and do not track the sun. Three types of collectors fall in this category:

1. Flat plate collectors (FPC)
2. Stationary compound parabolic collectors (CPC)
3. Evacuated tube collectors (ETC)

1.3.1.1. Flat-Plate Collectors (FPC)

A typical flat-plate solar collector is shown in Fig. 1. A simple flat plate collector consists of a flat surface called as absorber plate having high absorptivity for solar radiations [5]. When solar radiation permits through a transparent cover and imposes on the blacke – ned absorber surface of high absorptivity, a large portion of this energy is absorbed by the plate and then transferred to the transport medium in the fluid tubes to be carried away for storage or use. The underside of the absorber plate and the side of casing are well insulated to reduce conduction losses. The liquid tubes can be welded to the absorbing plate, or they can be an integral part of the plate. The liquid tubes are connected at both ends by large diameter header tubes [6]. Flat plate collectors are usually employed for low temperature applications up to 80°C [4].

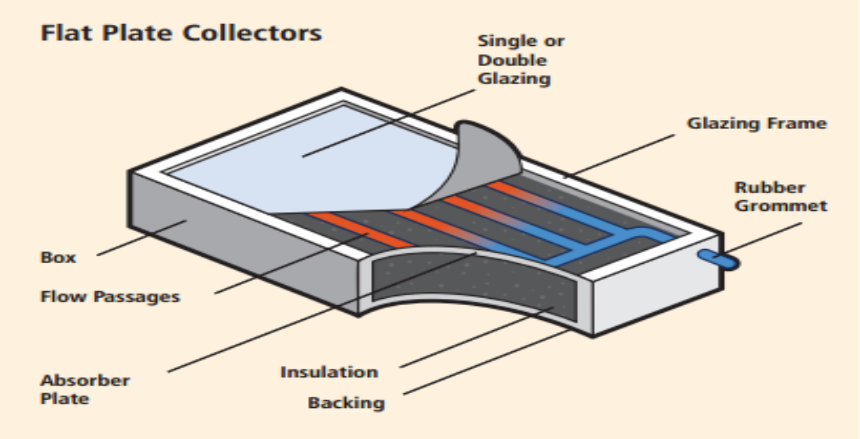

Figure 1 Schematic diagram of Flat-plate collector [7]

1.3.1.2. Compound Parabolic Collectors (CPC)

Compound parabolic collectors (CPC) have the capability of reflecting to the absorber all of the incident radiation within wide limits. The necessity of moving the concentrator to accommodate the changing solar orientation can be reduced by using a trough with two sections of a parabola facing each other, as shown in Fig. 2. Compound parabolic con centrators; can accept incoming radiation over a relatively wide range of angles. By using multiple internal reflections, any radiation that is entering the aperture, within the collector acceptance angle, finds its way to the absorber surface located at the bottom of the collector [4].

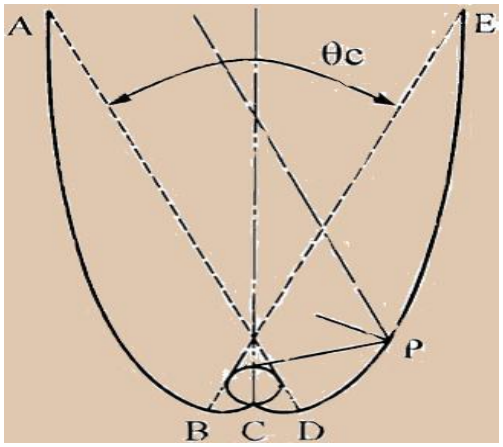

Figure 2 Schematic diagram of a CPC Collector [6]

1.3.1.3. Evacuated Tube Collectors (ETC)

Evacuated heat pipe solar collectors (tubes) consist of a heat pipe inside a vacuum-sealed tube, as shown in Fig. 3. Evacuated tube collectors have demonstrated that the combination of a selective surface and an effective convection suppressor can result in good performance at high temperatures. The vacuum envelope reduces convection and

conduction losses, so the collectors can operate at higher temperatures (~150°C). Both direct and diffuse radiation can be collected [6].

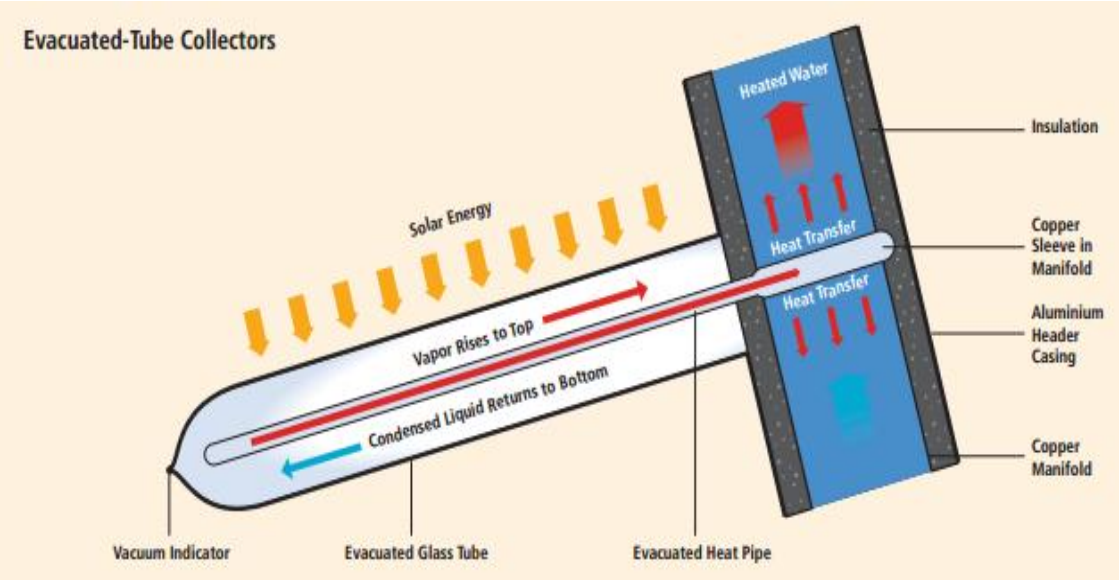

Figure 3 Schematic diagram of an evacuated tube collector [7]

1.3.2. Sun Tracking Concentrating Collectors

In concentrating collectors solar energy is optically concentrated before being transferred into heat. Concentration can be obtained by reflection or refraction of solar radiation by the use of mirrors or lenses. The reflected or refracted light is concentrated in a focal zone, thus increasing the energy flux in the receiving target [6].

The collectors falling in this category are:

1. Parabolic trough collector (PTC)
2. Linear Fresnel reflector (LFR)
3. Parabolic dish reflector (PDR) and
4. Heliostat field collector (HFC) or central receiver system

1.3.2.1. Parabolic trough collector (PTC)

Parabolic trough collectors are made by bending a sheet of reflective material into a parabolic shape. A metal black tube, covered with a glass tube to reduce heat losses, is placed along the focal line of the receiver as shown in Fig. 4. When the parabola is pointed towards the sun, parallel rays incident on the reflector are reflected onto the receiver tube. It is sufficient to use a single axis tracking the sun and thus long collector modules are produced. A glass cover tube is usually placed around the receiver tube to reduce the convective heat loss from the receiver, there by further reducing the heat loss coefficient.

Parabolic trough collectors (PTC) can effectively produce heat at temperatures between 50°C and 400°C for solar thermal electricity generation or process heat applications [4].

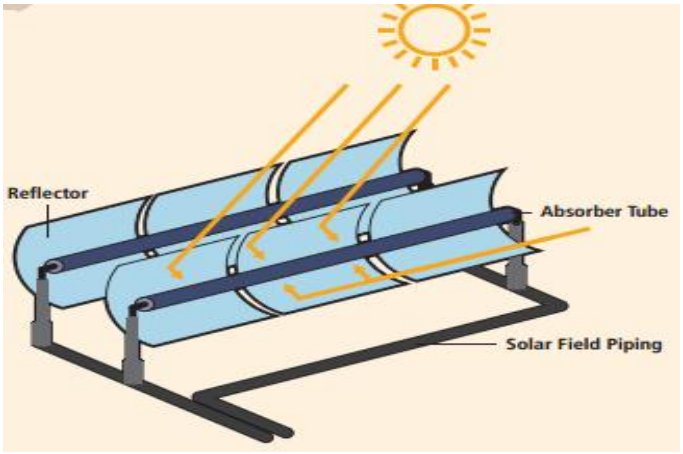

Figure 4 Schematic diagram of a parabolic through collector [7]

1.3.2.2. Linear Fresnel Reflector (LFR)

Linear Fresnel reflector (LFR) technology relies on an array of linear mirror strips which concentrate light on to a fixed receiver mounted on a linear tower. The LFR field can be imagined as a broken up parabolic trough reflector, but unlike parabolic troughs, it doesn't have to be of parabolic shape, large absorbers can be constructed and the absorber does not have to move. A representation of an element of an LFR collector field is shown in Fig. 5. The greatest advantage of this type of system is that it uses flat or elastically curved reflectors which are cheaper compared to parabolic glass reflectors. Additionally these are mounted close to the ground, thus minimizing structural requirements [6].

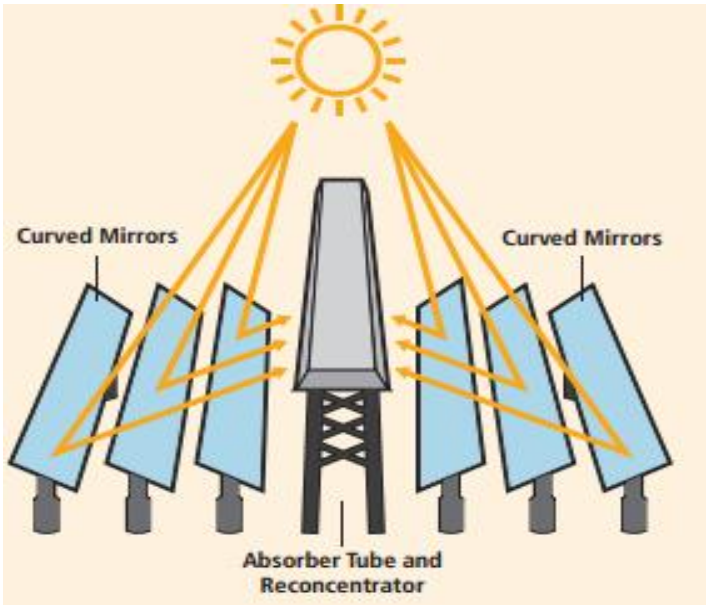

Figure 5 Schematic diagram of Linear Fresnel Reflector [7]

1.3.2.3. Parabolic Dish Reflector (PDR)

A parabolic dish reflector shown schematically in Fig. 6 is a point-focus collector that tracks the sun in two axes, concentrating solar energy onto a receiver located at the focal point of the dish.The dish structure must track fully the sun to reflect the beam into the thermal receiver. The receiver absorbs the radiant solar energy, converting it into thermal energy in a circulating fluid. The thermal energy can then either be converted into electricity using an engine generator coupled directly to the receiver, or it can be transported through pipes to a central power conversion system. Parabolic dish systems can achieve temperatures in excess of 1,500°C. Because the receivers are distributed throughout a collector field, like parabolic troughs, parabolic dishes are often called distributed receiver systems [6].

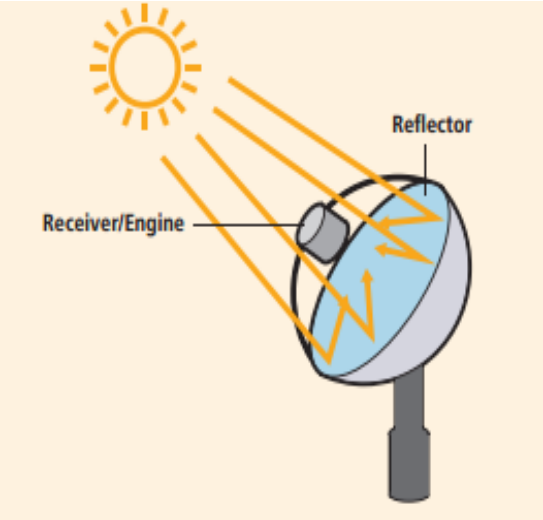

Figure 6 Schematic diagram of a parabolic dish collector [7]

1.3.2.4. Heliostat Field Collector (HFC)

For extremely high inputs of radiant energy, a multiplicity of flat mirrors can be used to reflect their incident direct solar radiation onto a common target as shown in Fig. 7. This is called the heliostat field or central receiver collector. By using slightly concave mirror segments on the heliostats, large amounts of thermal energy can be directed into the cavity of a steam generator to produce steam at high temperature and pressure. The concentrated heat energy absorbed by the receiver is transferred to a circulating fluid that can be stored and later used to produce power [6].

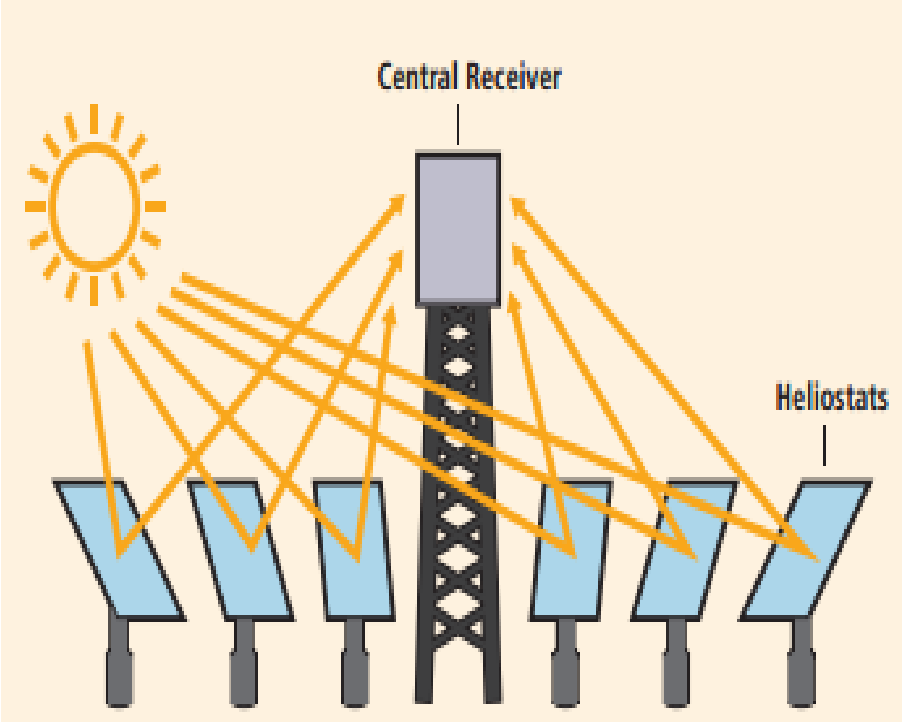

Figure 7 Schematic diagram of heliostat field collector [7]

1.4 SOLAR AIR HEATERS

Solar air heaters are one of the simplest and cost effective solar energy utilization systems, converts solar radiations into the useful thermal energy [8]. Air is used as a heat transfer medium in many of the energy conversion systems.

Solar air heaters have been made in variety of designs. In some of the absorber surface beneath the glazing includes overlapped, spaced, clear and black glass plates, single smooth metal sheets, flow through stacked screen or mesh, corrugated metal plates and others. In other air passing beneath the plate or underlying air passage reduces downward heat loss; and one or two covers of glass or transparent plastic provide resistance to upward convection and radiation losses. Flat plate collector forms the heart of any solar energy collection system. It is having the following advantage over the other type of collector of solar energy collectors [9]:

1. Absorb direct, diffuse and reflected components of solar radiation ,
2. Low cost and easy manufacturing
3. High efficiency
4. Fixed and no need of tracking
5. Long life and low maintenance cost

Classification of air heaters according to the absorbing surface are given below [9]:

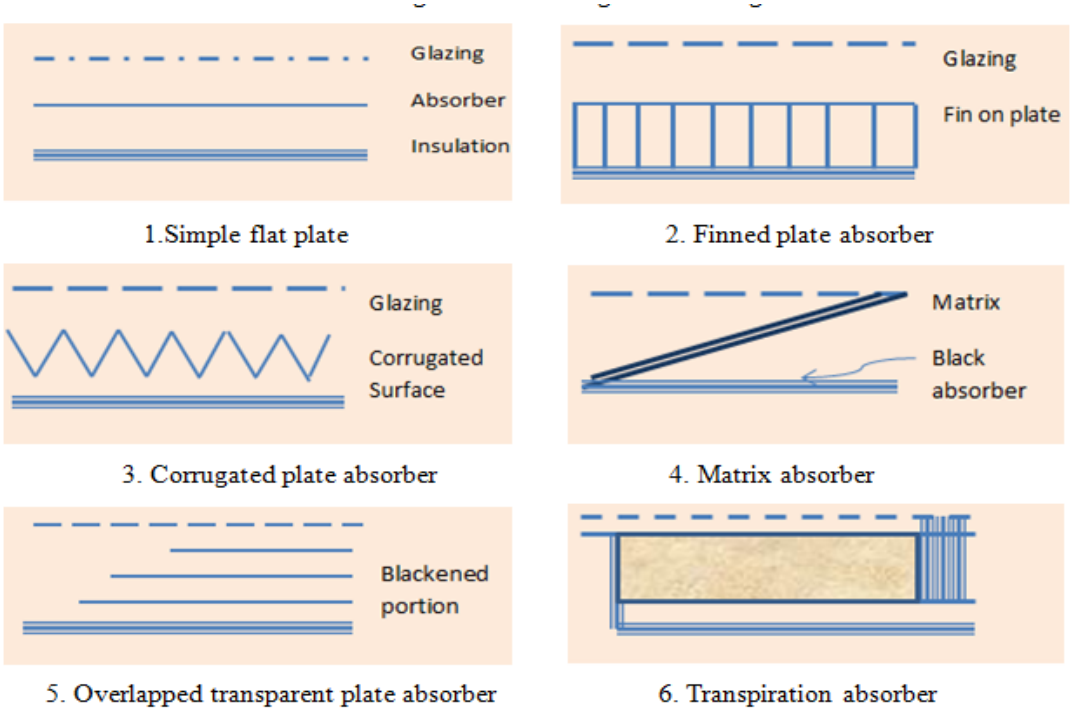

Figure 8 Classification of Air Heater [9]

1.5 PERFORMANCE OF AIR HEATER

Solar energy is one of the most promising and simply convertible forms of renewable energy on the earth. It requires proficient collection of energy and storage system for economical utilization. Cost effective solar energy utilization with the system of solar air heater, it converts the solar radiation into thermal energy which utilized by many applications. But the efficiency of solar air heater is very poor due to low heat transfer coefficient between the flowing air and absorber plate [10]. To increase the performances of air heater, artificial roughness geometry used on the absorber plate. Roughness is used to break the laminar viscous sub layer formed on absorber plate for increasing the level of turbulence to enhance the heat transfer.

There are following some technique to improve the performance of air heater [11]:

1.5.1 Reduction of heat losses

Heat loss is one of the main reason which results in lower heat transfer which further accounts for lower efficiency of the heater. So there is a need to minimize this heat loss so as to increase the properties of solar heater. Some of the ways of reducing heat losses from the solar collector are given below.

a) By lowering convective as well as irradiative heat losses

b) By selective absorber surfaces

1.5.2 Improvement of heat transfer from absorber plate

The low convective rate of heat transfer between the absorber plate and the air flowing in the duct, results in relatively high absorber plate temperature leading to higher heat losses to the environment. These losses can be reduced by lowering the absorber plate temperature by increasing the heat transfer coefficient between the absorber plate and the air flowing in the duct. This can be achieved by following methods:

a) By providing packed bed absorbers for solar air heating collectors
b) By increasing the area of heat transfer without effecting the convective heat transfer coefficient
c) By increasing convective heat transfer coefficient using artificial roughness.

CHAPTER 2 TERMINOLOGY

2.1 CONCEPT OF ARTIFICIAL ROUGHNESS

Artificial roughness is fundamentally a passive heat transfer technique by which thermohydraulic efficiency of solar iar heater is improved. The artifical roughness has been used extensively for the enhacement of forced convective heat tranfer, which furthe rquires flow at the heat transfer surface to be turbulent . Hence energy creating such turbulence has to come from the fan or blower and excessive turbulence leads to excessive power requirement to make air flow thriugh duct, so there is a need to minimize this power loss to make it more efficient [11].

Due to this roughness, turbulent boundary layer with small laminar sublayer to this roughness, turbulent boundary layer with small laminar sublayer is formed on the absorber plate. This laminar sublayer offer very high resistance to the heat flow. So by breaking this layer to create turbulence the heat transfer rate and Fr characteristics can be increased which So by breaking this layer to create turbulence the heat transfer rate and Fr characteristics can be increased which further increases the thermal efficiency and thermo hydraulic performance of a solar air heater. [11]

The key dimensionless geometrical parameters that are used to characterize roughness are [11]:

1. Relative roughness pitch (p/e)

Relative roughness pitch defined as the ratio of distance between two consecutive ribs and height of the rib.

2. Relative roughness height (e/D_h)

Relative roughness height (e/D_h) is the ratio of rib height to equivalent diameter of the air passage.

3. Angle of attack (α)

Angle of attack is inclination of rib with direction of air flow in duct.

4. Shape of roughness element

The roughness elements can be two-dimensional ribs or three dimensional discrete elements, transverse or inclined ribs or V-shaped continuous or broken ribs with or without gap. The roughness elements can also be arc-shaped wire or dimple or cavity or compound rib-grooved.

5. Aspect ratio

It is ratio of duct width to duct height. This factor also plays a very key role in investigating thermo-hydraulic performance.

CHAPTER 3 REVIEW OF LITERATURE

3.1 INTRODUCTION

The purpose of comprehensive literature review is to collection of particular articles, books and other sources about a specific subject. The purpose is to summarize the existing research that has been done in the present time and to highlight what research will add to the existing body of knowledge. Several methods used by many investigators to increase the efficiency. They are used different geometry and operating parameter which is summarized as literature review.

3.2. SINGLE PASS SOLAR AIR HEATER

Prasad and Saini [14] have investigated solar air heater with the use of small diameter protrusion wires on the surface of the plate which develop the expression Stanton number and friction factor.The results have been found to associate with mean deviation of 6.3 % for Fr and 10.7 % for the Nu.

Gupta et al. [15] studied that the thermohydraulic performance increased with the increase in insolation. For a roughened solar air heater, maximum enhancement in heat transfer and Fr was obtained to be of the order 1.8 and 2.7 times respectively at ‘α’ 60° and 70° respectively and the effect of (e/D_h), ‘α’ with respect to flow direction and Re on the thermohydydraulic performance of a roughned solar air heater for transitionally rough flow region which is shown in Fig. 9.

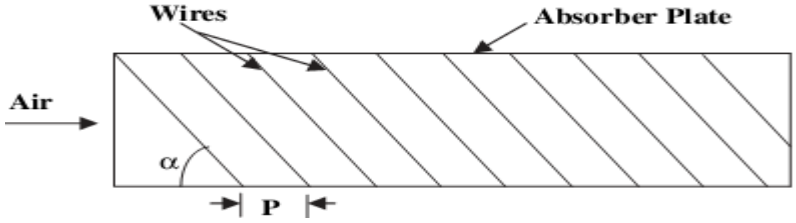

Figure 9 Configuration of inclined ribs [15]

L. Varshney and Saini [16] have done experimental investigations on heat transfer and fluid flow characteristics of a solar air heater having its duct packed with the wire mesh matrices. The investigation concealed a wide range of parameters of wire matrix geometry such as wire diameter, pitch, number of layers. They have developed correlation for heat transfer and

Fr coefficients for air flowing through the bed of wire mesh and also developed Colburn J-factor and friction factor. These correlations predict the experimental data with rational precision.

Ebrahim Momin at al. [17] examined the effect of V-shaped ribs on heat transfer and fluid flow characteristics on the absorber surface of plate. It was obtained the maximum performance at angle of attack of $60^{0.}$.

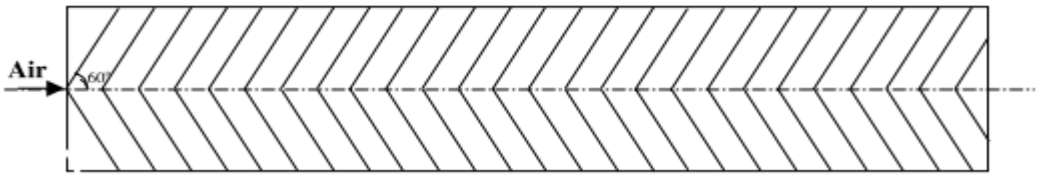

Figure 10 Configuration of V-shaped ribs [17]

Bhagoria et al. [18] examined the impact of wedge shape roughness on the heat transfer and friction factor of absorber plate used in the solar air heater. The range of Re is from 3000 to 18000, (e/D_h) is from 0.015 to 0.033, (p/e) is from 6 to 12.12 and wedge angle ϕ is from 8 to 15°. It was also observed that the Nu increases 2.4 times as that of the smooth duct and friction factor 5.3 times.

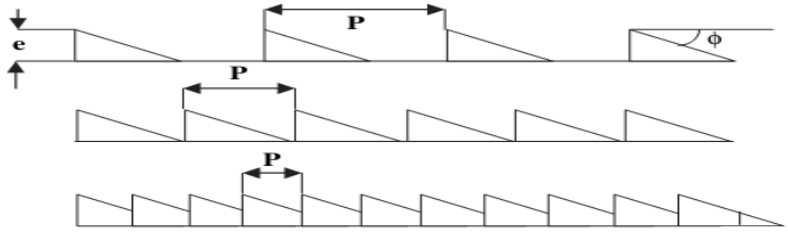

Figure 11 Configuration of wedge shape roughness [18]

Togrul et al. [19] investigated the development and analysis of solar air heater with conical concentrator. They studied the performance of solar air heater with a cylindrical absorber centered to a conical concentrator for focusing incident solar radiation. There primary objective was to attain higher temperatures than that of the flat plate collectors. They found that tilting angles under local latitude would be most appropriate for collector installations and can attain a temperature of 150 ^{0}C.

Sahu and Bhagoria [20] have probed the impact of 90˚ transverse broken ribs in Fig. 15 on the heat transfer coefficient using the roughness parameters and flow parameter like (p/e) of 10 to 30 mm, rib height of 1.5 mm, aspect ratio for the duct of 8 and Reynolds number between 3000-12,000. It was found that Nusselt number attains the maximum value at the

roughness pitch 20 mm and goes on decreasing with increase in roughness pitch. Roughness on the absorber plate increases the heat transfer coefficient by 1.25-1.4 times as that of the smooth duct.

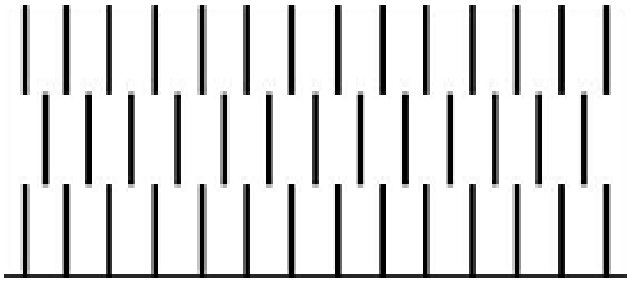

Figure 12 Configuration of broken transverse ribs [20]

Singal et al. [22] examined the heat transfer and Fr characteristics. The variation of Re number from 2000 to 14000, relative roughness pitch (p/e) 3 to 8 and relative roughness height (e/D_h) 0.0030. The maximum thermal efficiency of air heater at (p/e) is 8.

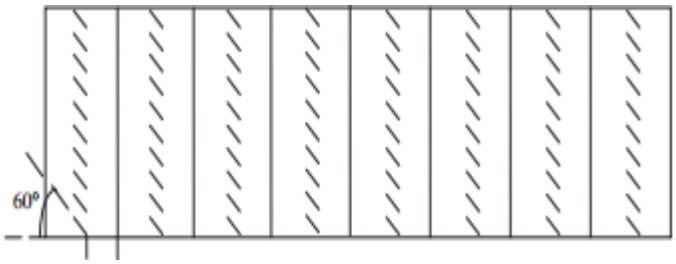

Figure 13 Configuration of inclined and transverse ribs [22]

Aharwal et al. [23] examined the effect of geometrical parameter of gap width and gap position Fig. 14. They have observed that maximum enhancement in heat transfer and Fr occur at relative gap position of 0.25, relative gap width of 1.0, relative roughness pitch (p/e) of 8.0, angle of attack (α) of 60° and relative roughness height (e/D_h) of 0.037. Based on the experimentation correlation for the Nusselt number and friction factor have been developed.

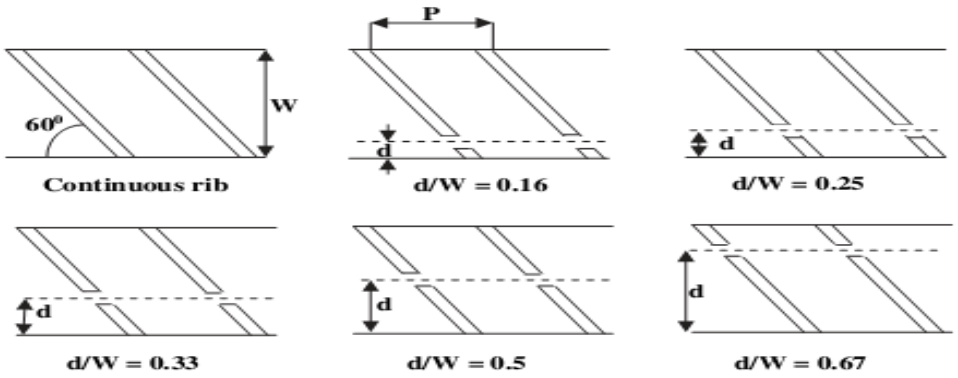

Figure 14 Configuration of inclined rib with gap [23]

Prasad et al. [24] investigated on a packed bed solar air heater using wire mesh. The range of air mass flow rate is 0.0159 to 0.0347kg/s-m^2. They developed the correlation for Colburn J_h factor and Fr as function of the parameter of Reynold number and bed. The bed with the lowest value of porosity has the best thermal performance in between 53.3% to 68%.

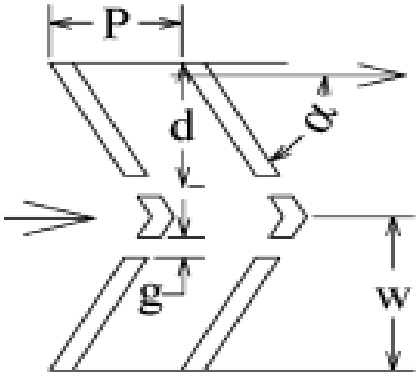

Figure 15 Configuration of discrete downward V ribs [25]

Bhushan et al. [26] gave the Nu and Fr correlations for solar air heater duct having artificially roughened absorber plate. They find out an investigational study in order to analyze the influence of artificial roughness in a solar air heater having protrusions as roughness geometry Fig.16.

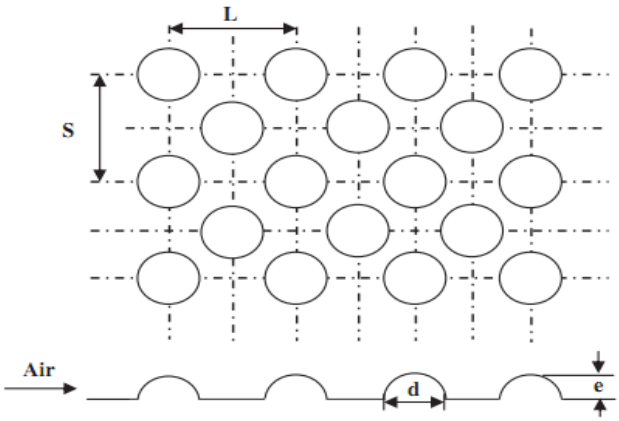

Figure 16 Roughened geometry on absorber surface [26]

3.3. DOUBLE PASS SOLAR AIR HEATER

Satunanathan and Deonarine [27] presented the concept of counter flow of DPSAH. The air flows between absorber plate and glass cover and then get induced into the duct. It was found that the efficiency of two pass solar air heater is 10-15% more efficient than the single pass solar air heater.

Figure 17 Schematic diagram of double pass air heater [27]

N.E. Wijeysundera et al. [28] studied the thermal performance of two-pass solar air heaters. He found that the procedure of a predictable solar air heater with two covers in a two pass mode offers an economical method of enlightening the collector effectiveness by 10-15%. They also developed models for two-pass flow arrangements and associated with the performance of a single pass design.

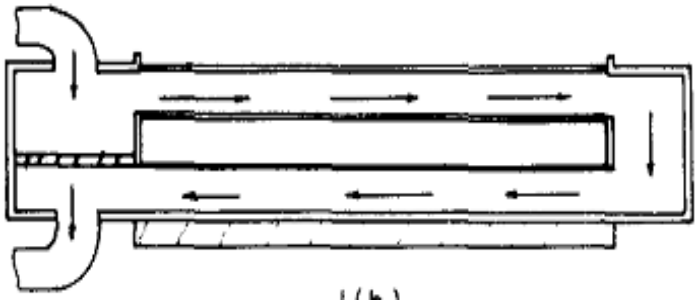

Figure 18 Schematic diagram of double pass air heater [28]

N. K. Bansal et al. [29] analyzed a non–porous element on the absorbing surface in DPSAH. From the analysis, an expression for the outlet temperature and useful heat flux has been obtained in terms of mass flow rate and other relevant parameter. The efficiency of air heater increases due to use of double glazing for small mass flow rates.

A. A. Mohamad [30] has given the concept to diminish the heat losses from the front cover of the collector and to get the most out of heat extraction from the absorber using the porous absorber to improve the heat transfer. The thermal efficiency of the suggested collector exceeds 75% under normal operating conditions and flow rate of air varies from 0.002 to 0.2 kg/(ms).

K. Sopian et al. [31] had designed for different working situation of collector with or without porous media. They obtained numerous significant relations between the design and different working conditions. They obtained that performance about 20-70% higher than others.

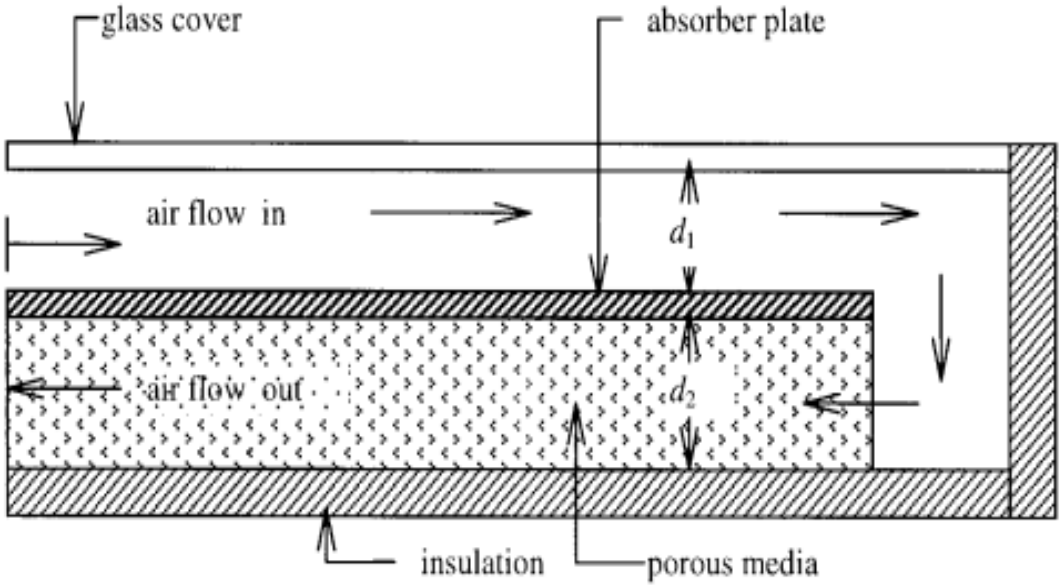

Figure 19 The schematic of a double-pass thermal solar collector with porous media in the second layer [31]

H.M. Yeh et al. [32] studied both experimentally and analytically of collector efficiency with fins attached on both side of absorbing plate. It shows that the collector efficiency is unity i.e. the optimal fraction of airflow rate r, is 0.5. The thermal performance reduces when r, as well as (1-r), goes away from 0.5. The collector efficiency of air heater is 70.5% at the value of r is 0.5. It obtained that the collector efficiency is improved by providing of fins.

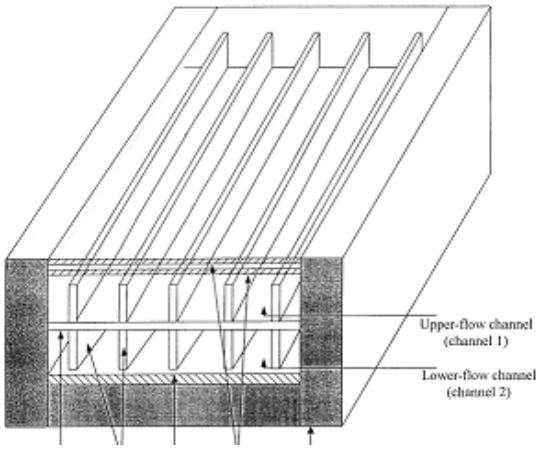

Figure 20 DPSAH with fins attached [32]

Dilip and Rajeev [33] have analyzed the analytical model for an inclined multi pass solar air heater within built thermal storage on deep- bed dryer. The drying rate and humidity of the air rises with the increase in the depth of drying bed. The design parameter of collector are L=4m, b=1m, $\beta = 30^0$ and mass flow rate is 2.8×10^{-2} kgs^{-1}.

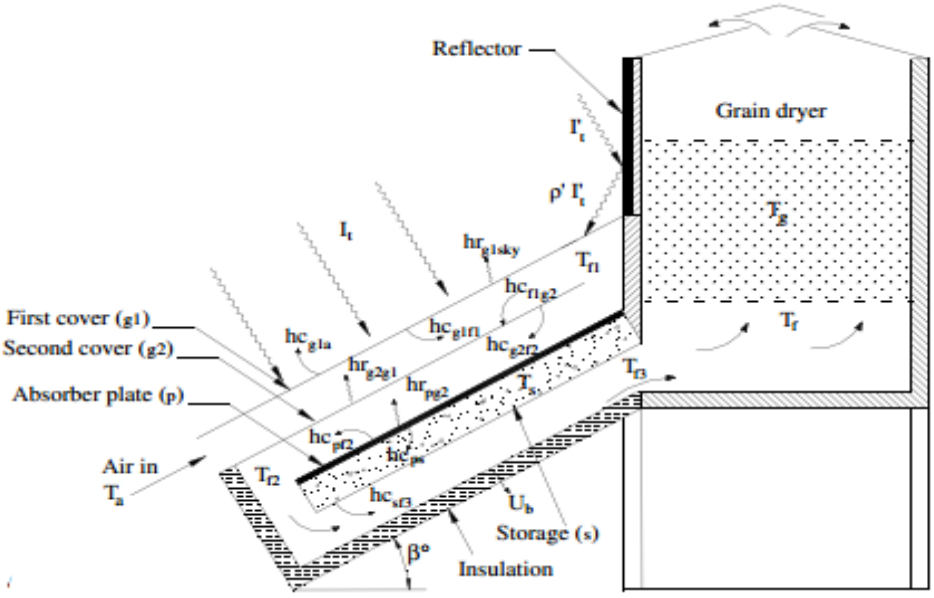

Figure 21 Multi pass air heater with deep bed drying system [33]

Paisarn Naphon [34] examined the heat transfer characteristics and the act of air heater by the mathematical modeling. The model is validated by comparing with the experimental data of K. Sopian et al. [31]. Naphon [35] also performed in the entropy generation which have longitudinal fins in solar air heater. He did his experiment with mass flow rate ranging between 0.02 kg/s to 0.1 kg/s.

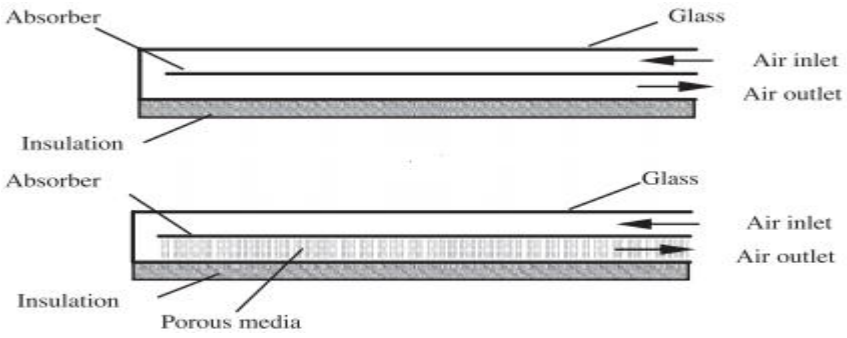

Figure 22 Schematic diagrams of the solar air heaters without and with porous media [34]

El-Sebai et al. [36] examined the thermal performance in double pass solar air heater. It is recommended to operate the system with packed bed with values of mass flow rate 0.05 kg/s or lower having a pressure drop across the air heater. The maximum value of solar radiation intensity is 878 W/m^2. It was found that the thermohydraulic efficiency increase with increasing mass flow rate. While thermohydraulic efficiency with limestone or gravel as packed bed is higher than that without packing by about 25.6% and 28.3% respectively.

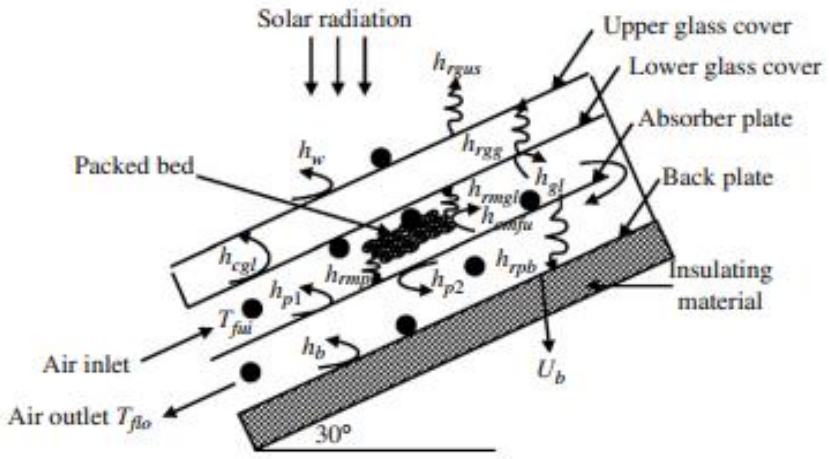

Figure 23 A schematic diagrams of the system and thermocouple positions [36]

Hikmet Esen et al. [37, 38] investigated a device for inserting an absorbing plate made of aluminum cans into the double pass channel in a flat plate solar air heater. Three different absorber plates had been designed and tested which helps to improve the efficiency. The highest efficiency of plate first is high than other at the mass flow rate of air is 0.05kg/s.

A.P.Omojaro et al. [39] have investigated that use of wire mesh as an absorber surface, the thermal efficiency of single and double pass solar air heaters increases when the mass flow rate increases from 0.012 kg/s to 0.038 kg/s. They also found that the maximum thermal efficiency obtained is 59.62% and 63.74% for both single pass and double pass solar air heater respectively for air mass flow rate of 0.038 kg/s.

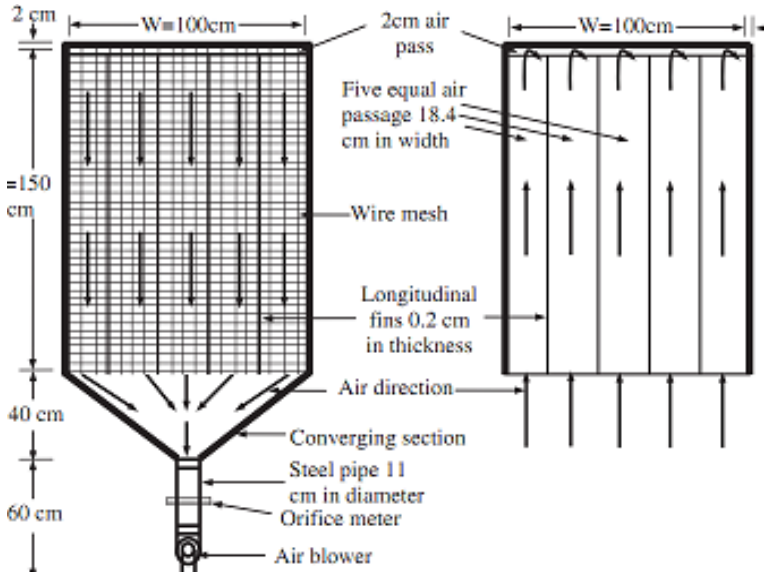

Figure 24 Single and double pass solar air heating [39]

Rakesh and Marc [42] have investigated on a photovoltaic/thermal solar air heater and vertical fins in DPSAH. The effects of design, climatic and functional parameters are calculated on thermal, , cell temperature, outlet air temperature and electrical efficiency and total equivalent thermal energy. The thermal and electrical efficiency added about 15.5% and 10.5% respectively due to attachment of fins.

Chii-Dong Ho et al. [44] carried out an exploration of collector efficiency of upward-type with fins attached. They found that collector efficiencies increases with increasing mass flow rate and fins attached. He also found that collector efficiency is improved by 76.17% and 81.27 % by using the recycling operation.

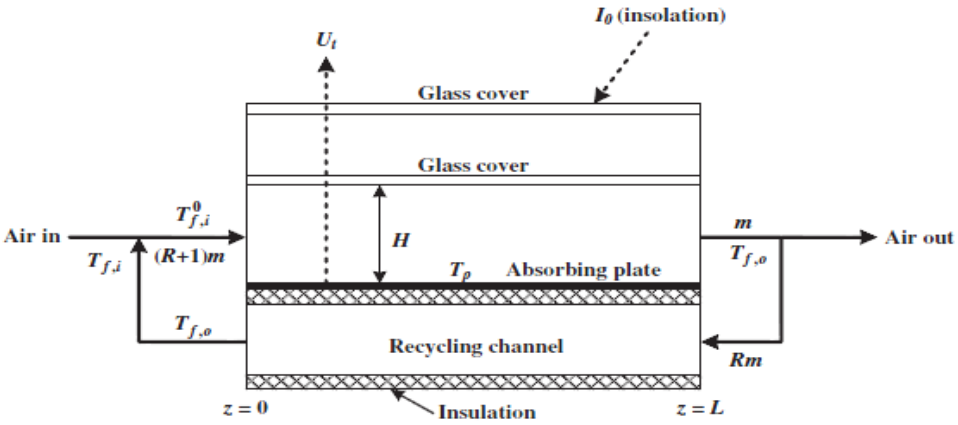

Figure 25 Section view [44]

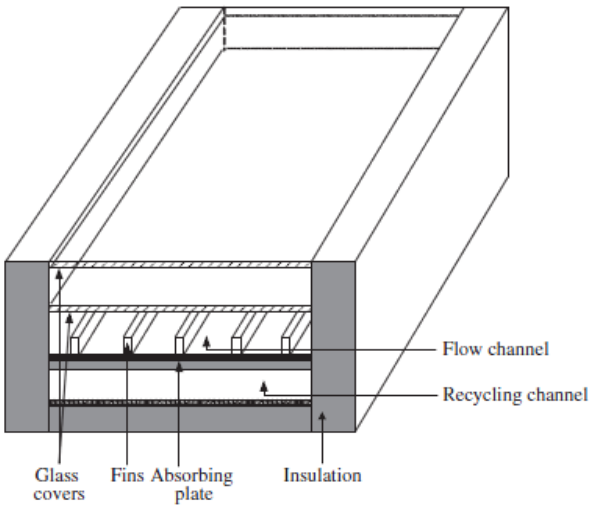

Figure 26 Fins attached on plate [44]

Shalaby et al. [45] investigated the thermal performance of double pass finned solar air heater. He did his investigation both theoretically and experimentally. The results showed that the v-corrugated plate solar air heater is 9.3–11.9% more efficient compared to the finned plate

solar air heater. Mass flow rates used were o.0125-0.0225 kg/s. So from his study it is observed that the double pass solar air heater is preferably a better choice than a single pass solar air heater and double pass is always more efficient than a single pass solar air heater. Shalaby et al. [46] carried out both experimentally and theoretically on v corrugated plate in double pass solar air heater. They obtained that the efficiency of double pass v-corrugated solar air heater is 11-14% higher than the double pass flat plate solar air heater. During the higher efficiency mass flow rate is 0.02kg/s.

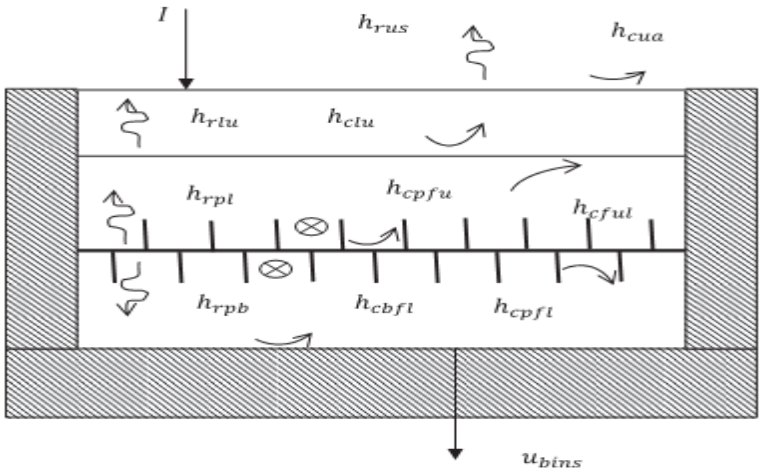

Figure 27 Double pass finned solar air heater [46]

Sudhanshu [47]has performed an experimental study on a Double pass solar air heater having rectangular duct. Three valves of rectangular duct is kept insulated, a uniform heat flux is provided on one side of duct that is the absorber plate. The aspect ratio of the Duct (WH)is 10. The range of Reynolds number varies from 4900 to 12000. The relative rough – ness pitcis between 5 to 20 and fixed relative roughness height (eDh)is 0.044 and fixed angle of attack is 90°. It has been observed that maximum heat transfer and friction factor occur at relative roughness pitch (p/e) of 10

.

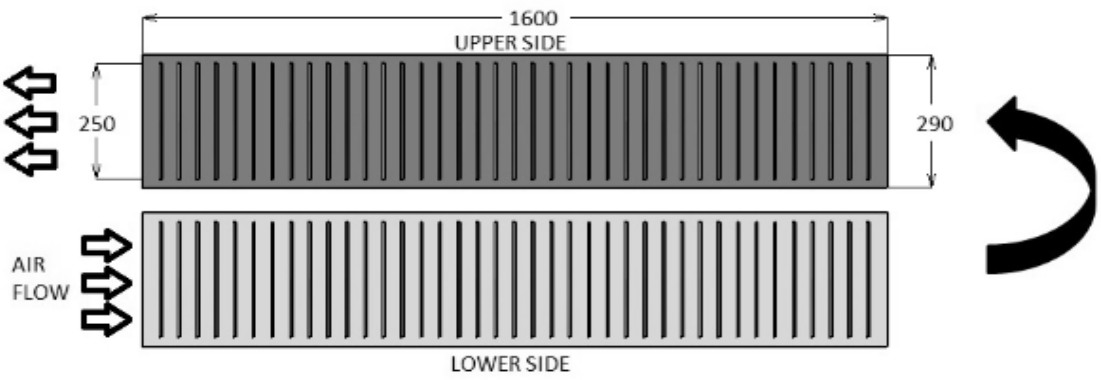

Figure 28 Absorber Plate

Prsashant and Satyender [48] investigated the analytical model to predict the thermal and thermohydraulic efficiencies of different design of model A and model B in double pass packed solar air heater under the external recycle. The recycle ratio and mass flow rate of model A and model B are varied from 0.1 to 1 and 0.01 to 0.025 Kg/s respectively. The maximum value of the thermal efficiency of model A is obtained 80.8 % which is about 13% higher than that of model B at mass flow rate of 0.025kg/s, the recycle ratio is of 1 and the channel depth ratio is of 3, respectively.

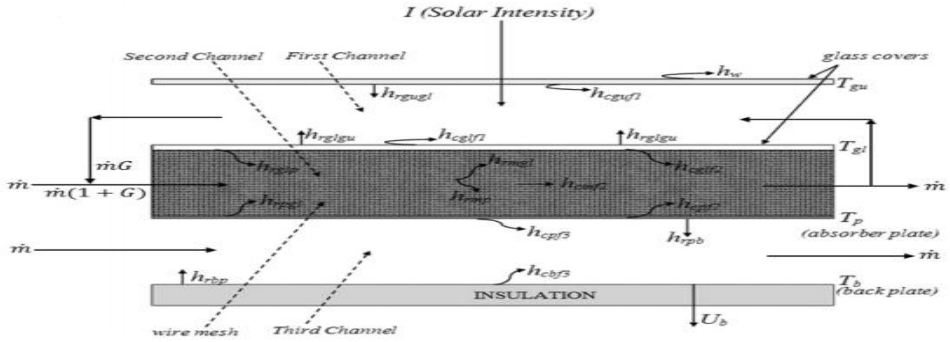

Figure 29 Various heat transfer coefficients for Models [48]

CHAPTER 4 RATIONALE AND SCOPE OF STUDY

2.1 INTRODUCTION

The major application of air heater as crop drying, space heating, production plants, factories, workshops, warehouses, exhibition halls, offices, institutional facilities, theaters, gymnasiums, dryers, cleaners etc. in fact, in all places where a heating system, make-up air unit and ventilation system of air heater to space heating, crop drying food dehydration etc. [2, 49] . The aim of this study to find out the effect of discrete ribs on the absorber plate on heat transfer and friction factor characteristics and analyze the range of system and operating parameter of artificial roughness due to the geometry of ribs. The performance of solar air heater can be enhanced in many ways which is given below:

2.3. SCOPE OF STUDY

i. Study of double pass solar air heater integrated with ribs on upper and lower side of absorber surface of plate is done.
ii. Discrete ribs as roughness element on the absorber plate is better and give quality results as compared to continuous ribs with different geometry like wedge shape, V shape, W shape etc.
iii. By taking different parameters of Double pass solar air heater from the experimental work, mathematical model may be developed.
iv. With the help of experimental reading we can make the CFD modeling and also validate it for smooth plate and plate with ribs mounted on it.
v. There is a lot of scope of flow visualizations over selected roughness geometry by using the flow visualization technique.
vi. To investigate the theoretical humidification-dehumidification desalination system configured by a double pass solar air heater and also finds out the entropy generation in air heater system.
vii. By increasing its efficiency to its maximum limit it can be used for industrial applications for crop drying, space heating etc. which reduce the cost and energy of the system.

CHAPTER 5 OBJECTIVES OF THE STUDY

5.1 RESEARCH GAP

The study of literature review, it is observed that the efficiency of solar air heater is low due to low convective heat transfer between the absorber plate and the fluid flowing inside the duct. So to increase the thermal efficiency of solar air heater many investigators do many experiments. Several methods have been used by various investigators to increase efficiency. Some of them are use of artificial roughness on absorber plate, use of fins, electro hydrodynamic method, packed bed etc. Out of these the easiest and most acceptable method to enhance the heat transfer is the creation of artificial roughness on the absorber plate of solar air heater.

Various investigators studied thermal and thermohydraulic efficiencies, and heat transfer and friction loss by attached by ribs on absorbing plate of different shape size and orientation. Some of the artificial roughness element on absorber plate as given below which was used in single pass solar air heater or double pass solar air heater:

- Transverse rib
- Transverse broken ribs
- Inclined continuous ribs
- Inclined rib with gap
- V- shaped rib
- Discrete V-shaped rib
- Multi V-Shaped rib
- Transverse and inclined rib
- Arc shaped rib
- U- Shaped rib
- W-shaped rib
- Discreet W-shaped ribs
- Z-shaped rib

Out of the given above different types of geometry on absorber plate that only transverse ribs performed in double pass solar air heater for thermal and thermohydraulic efficiencies by Sudhanshu [47], so we decided that the artificial roughness of discreet ribs on the absorber plate at different angle of attack, relative roughness height and relative roughness of pitch.

5.2 OBJECTIVE OF STUDY

1. To study of roughness geometry provided on absorber plate of solar air heater.

2. To identification of new roughness geometry for absorber plate.

3. Experimental investigation performance of a roughened solar air heater based on thermal efficiency, thermo-hydraulic efficiency, for various values of Reynolds number, for selected artificial roughness geometry.

4. Investigate and study the performance of solar air heater by relative roughness height, relative roughness pitch and angle of attack.

CHAPTER 6 RESEARCH METHODOLOGY AND EXPERIEMENTAL SETUP

6.1 INTRODUCTION

Solar air heater is a renewable energy heating technology use to heat or condition air for building or heat process application. Solar air heater is the simplest device which is use to convert the solar energy into heat energy.

In order to obtain the experimental data for the design, manufacturing and installation data of experimental setup for double pass solar air heater. Artificial roughness has been created by using ribs of wire. The ribs are attached on the absorber plate to produce different orientations like V shape, W shape, inclined, transverse ribs, etc.

6.2 RESEARCH METHODOLOGY

There are three methodologies which can be used to enhance the performance of the system and heat transfer characteristics which are given below:

- Experimental
- Theoretical
- Computational

Present work is concerned about the experimental research methodology and further categorized into the following steps

- CAD modeling of Experimental Setup
- Manufacturing of Experimental Setup
- Selection of Roughness Geometry
- Experimentation
- Verification of 'Dittus-Boelter' and 'Blasius' equation for Smooth Plate
- Comparison of the results of Roughened Absorber Plate with that of Smooth Plate
- Thermal Performance
- Thermohydraulic Performance

Flow chart of research methodology is given below:

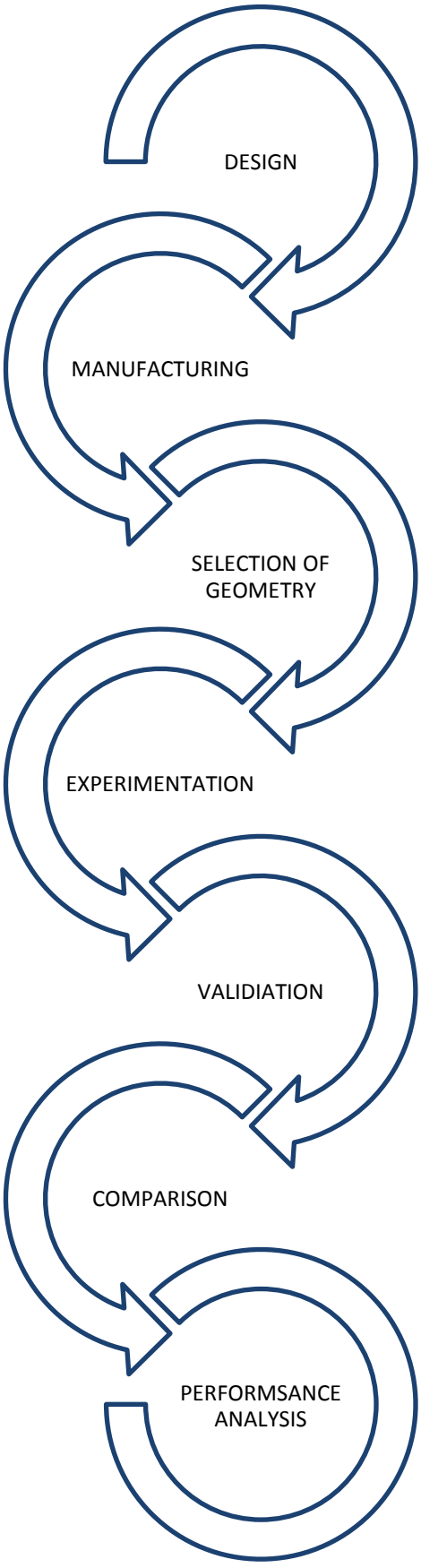

6.3 DESCRIPTION OF EXPERIMENTAL SETUP

Experiments are conducted with DPSAH, the schematic diagram of experimental setup is shown in Fig. 31 and pictorial view of complete setup is shown in Fig. 32.

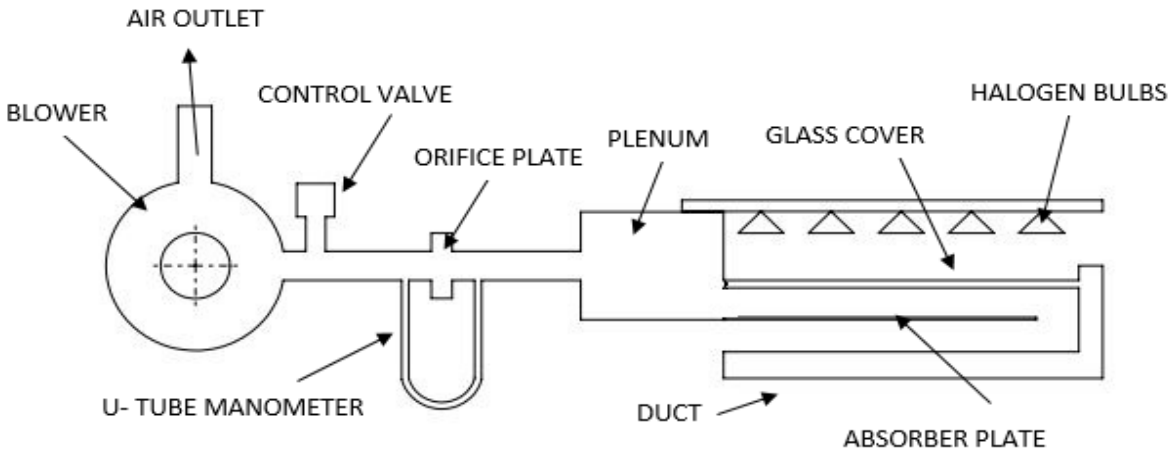

Figure 30 Schematic diagram of experimental setup

Figure 31 Pictorial view of experimental setup

6.3.1 Suction Air Blower and Control Valve

A suction air blower of 3 HP, 3000 rpm and 230V three phase power supply is used in experimental setup for suction of atmospheric air is shown in Fig. 33 and galvanized iron pipe of 80 mm internal diameter and length of 1500 mm used for connecting the blower to plenum and duct. Two valves are provided, one at entrance and other at exit of blower for precise control of air flow rate. All parts are assembled and sealed with the help of gasket and sealant, in order to avoid air leakage.

Figure 32 Suction air blower and control valve

6.3.2 Orifice Plate

An orifice plate is placed between two pipes which connect the suction air blower and plenum as shown in Fig. 34. An orifice plate of 80 mm inlet pipe diameter, 4 mm thickness and 45^{o} edge angle. The mass flow rate of orifice has been measured with the help of calibrated orifice plate and also pressure drop across orifice plate has been measured with the help of U-tube manometer.

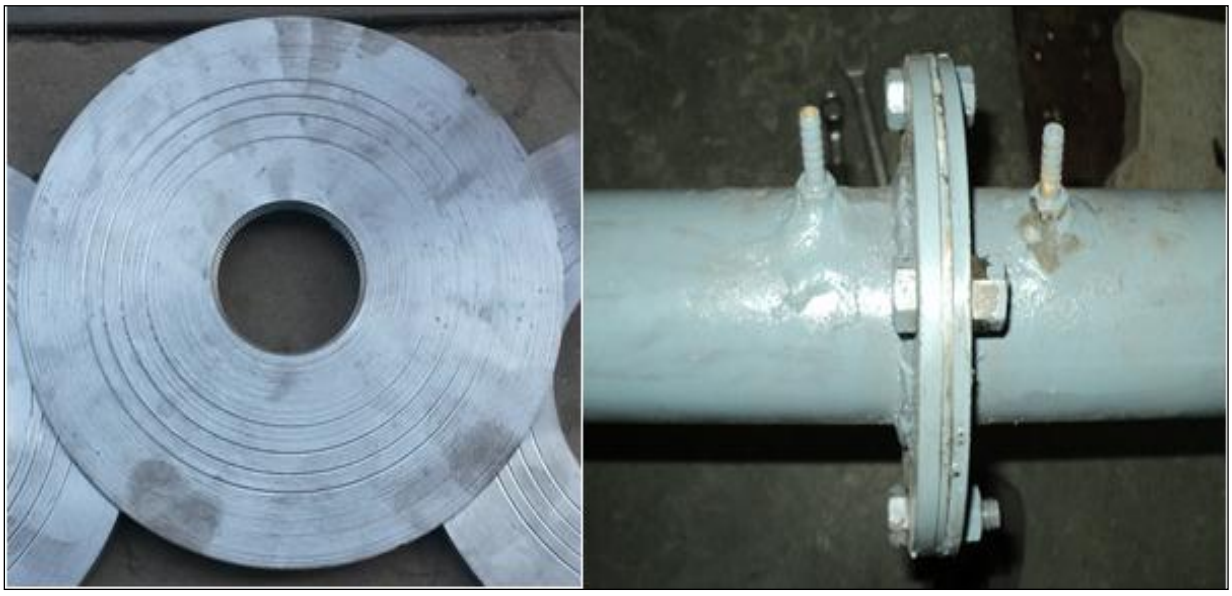

Figure 33 Orifice plate assemble

6.3.3 Solar Simulator

A solar simulator is use to provide constant heat flux to absorber plate through glass. Solar simulator is use to simulate spatial and spectral distribution of solar radiations into a focal plane which act as a highly concentrate solar system. The intensity of radiation is measured with the help of pyrometer, which is consists of six 500 W of halogen lights. Pictorial view of solar simulator is shown in Fig. 35.

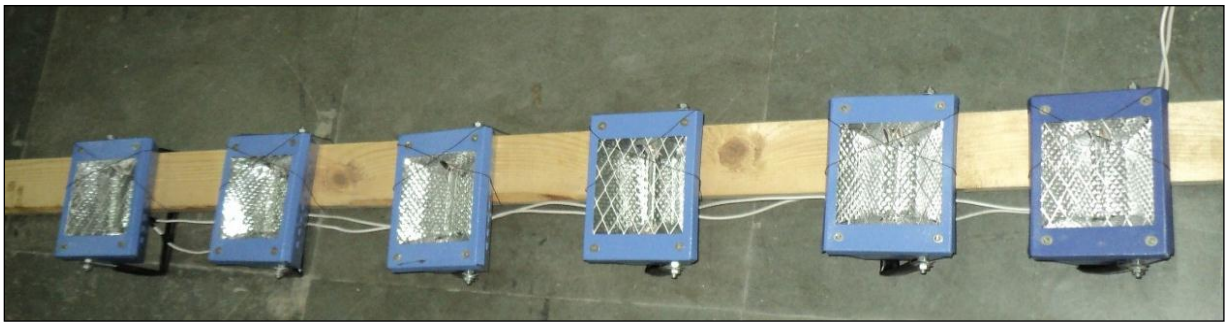

Figure 34 Solar Simulator consists of six halogen lights

6.3.4 Solar Air Heater Duct

CAD model and sectional view of double pass solar air heater are shown in Fig. 36 and Fig. 37 respectively. The dimension of duct is 2070 mm × 250 mm × 25 mm and the aspect ratio of duct is 10. The length of test section is 1600 mm and entry length is 400 mm. A space of 70 mm is left out at the end, for the movement of air towards upper duct and the duct is designed as per ASHARE standard [51]. The length of the entry section is given by $5\sqrt{WH}$. The duct is manufactured from the wooden plank of rectangular cross section which is shown in Fig. 38.

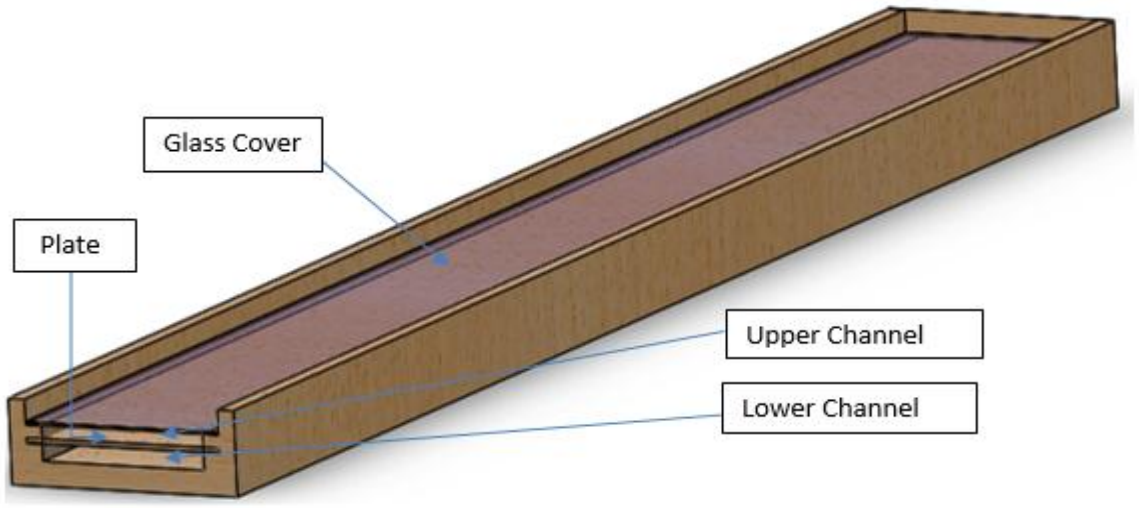

Figure 35 Schematic 3-D view of solar air heater

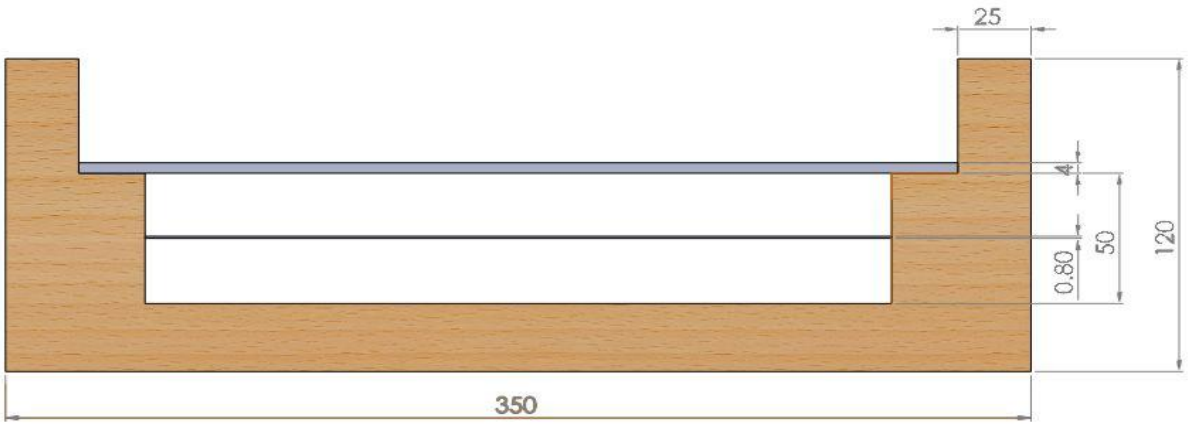

Figure 36 Schematic sectional view of duct

Figure 37 Pictorial view of solar air duct

6.3.5 Roughened Absorber Plate

A schematic diagram of discrete roughened absorber plate is shown in Fig. 39. A galvanized iron sheet has been used as an absorber plate. The size of the galvanized iron absorber plate is 1600 mm × 250 mm, artificial roughness has been provided on both side of the absorber plate in the form of discrete inclined ribs of aluminum wire of 2 mm diameter. The absorber plate was heated from upper side with the help of the solar simulator and thus subjected to uniform heat flux. There are different parameters of roughness absorber plate such as relative roughness height, relative roughness pitch and angle of attack. A pictorial view of

discrete ribs on upper side and lower side of absorber plate at different angle of attack 90°, 60° and 30° are shown in Fig. 40, Fig. 41 and Fig. 42 respectively.

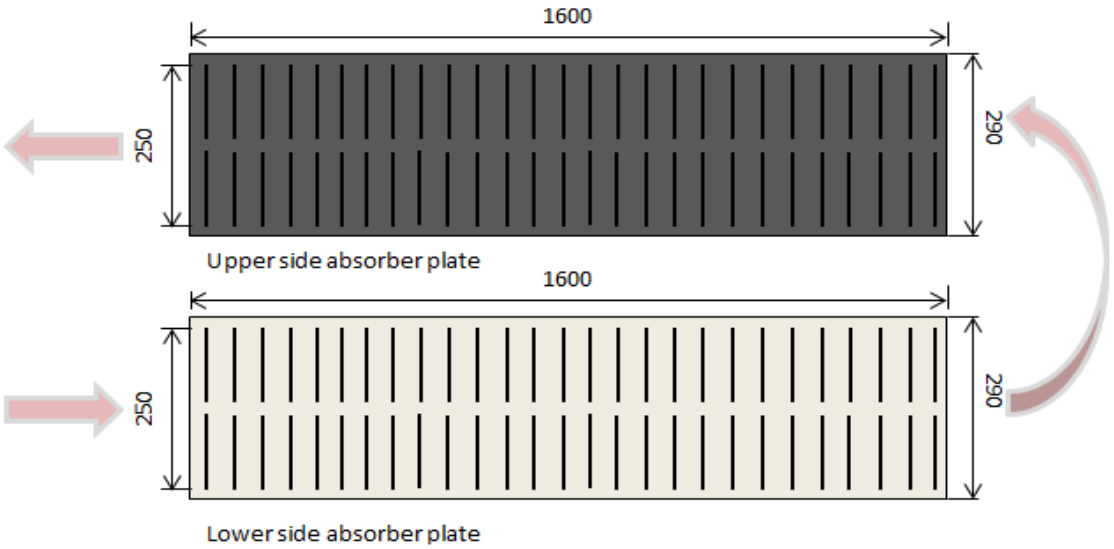

Figure 38 Schematic diagram of absorber plate

Figure 39 Pictorial view of absorber plate at angle of attack 90°

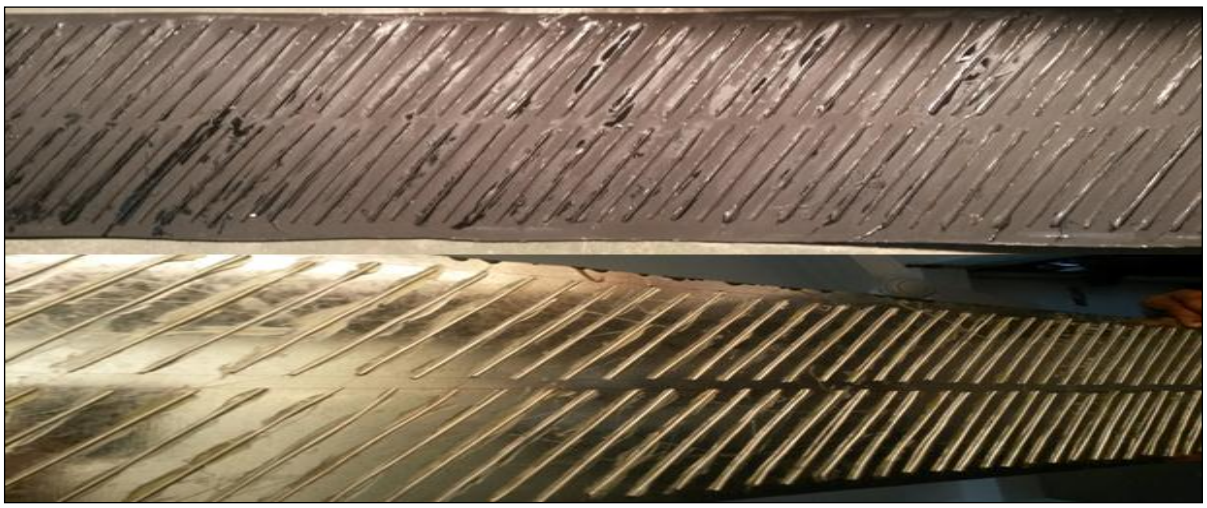

Figure 40 Pictorial view of absorber plate at angle of attack 60°

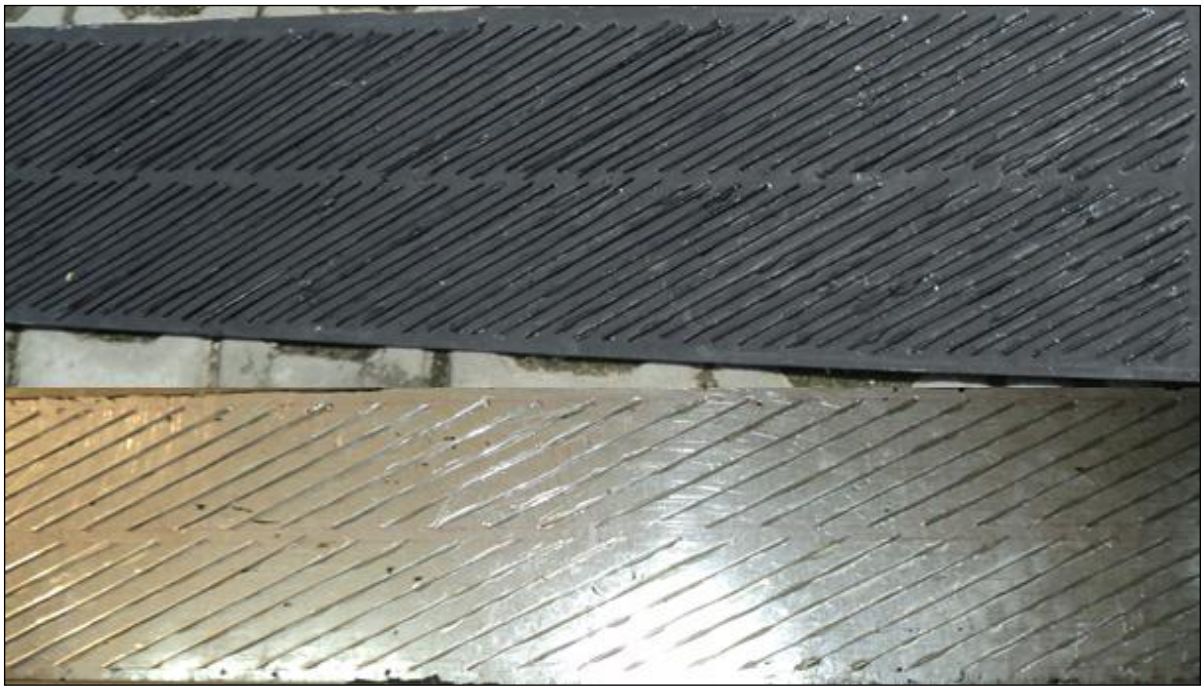

Figure 41 Pictorial view of absorber plate at angle of attack 30°

6.4 EXPERIMENTAL PROCEDURE

Experimental set-up runs under quasi-steady state condition for collecting heat transfer and friction factor data. Control valve is used to achieve the desire mass flow rate. There are various numbers of joints, which should be check for leakages are as follow: duct joints, inlet and outlet section of duct and pipe fittings. The following data were recorded:

- The temperature of absorber plate at 12 different locations on the absorber plate and air temperature at inlet and outlet of test section of duct.
- Pressure drop across the test section.
- Pressure measurement across the orifice meter.

6.4.1 Instrumentation and Data Reduction

Step.1 Mean Plate and Air Temperature: In this section precision temperature of entry level, exit level and absorber plate are measured by using 10k-ohm NTC thermistor with the help of simple digital multimeter and calculated. There are twelve thermistor mounted at absorber plate which is shown in the Fig. 43, while extra thermistor for inlet and outlet of test section are also provided. The mean plate temperature 'T_p' is calculated by the average of temperatures recorded at various locations on absorber plate, formulae for the same given below

$$Tp = \frac{T1+T2+T3+T4+T5+T6+T7+T8+T9+T10+T11+T12}{12} \qquad 6.1$$

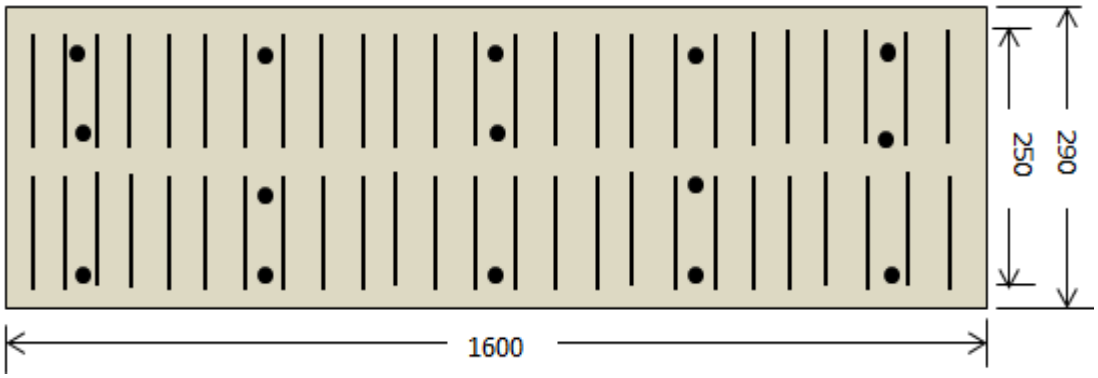

Figure 42 Location of temperature sensor

The bulk mean air temperature, 'T_f' is the arithmetic mean of measured values of air temperature at the entry and exit of the test section, formulae for the same given below

$$T_f = \frac{T1+T2}{2} \qquad 6.2$$

Step.2 Mass Flow Rate of Air: A U-Tube manometer had been used to measure the pressure drop across the orifice plate and orifice plate is used to measure mass flow rate of the air; as

$$m = C_d A_0 \sqrt{\frac{2\rho(\Delta P)}{1-\beta^4}} \qquad 6.3$$

Step.3 Velocity of Air through Duct: The velocity of air is calculated from the knowledge of mass flow rate and area of flow i.e. the cross section area of the duct as,

$$V = \frac{m}{\rho WH} \qquad 6.4$$

Step.4 Hydraulic Diameter: The hydraulic diameter of the rectangular section of the duct is determined from the relationship as given below,

$$D_h = \frac{4A_c}{P} \qquad 6.5$$

Step.5 Reynolds Number (Re): The Re of airflow in the duct is calculated from the following relationship,

$$Re = \frac{\rho V D_h}{\mu} \qquad 6.6$$

Step.6 Friction Factor (f): A projection manometer having least count of 0.01 mm was used to measure the pressure difference across the test section. Pressure drop (ΔP) is used to find out the Fr using equation as;

$$f = \frac{2(\Delta P)D_h}{4\rho L V^2} \tag{6.7}$$

Step.7 Heat Transfer Coefficient (h): The heat transfer coefficient is calculated from the relationship given below as;

$$h = \frac{Q_u}{A_p(T_p - T_f)} \tag{6.8}$$

Whereas T_p and T_f are the mean absorber plate and the fluid temperatures respectively, as discussed above and Heat transfer rate (Q_u) to the air is given by as;

$$Q_u = mC_p(T_O - T_i) \tag{6.9}$$

Step.9 Nusselt Number (Nu): The heat transfer coefficient calculated using the above equation is used to determine the Nu as given below as;

$$Nu = \frac{hD_h}{k} \tag{6.10}$$

Step.10 Thermal Efficiency: The concentration of light *'I'* is measured with the help of pyrometer. Calculation of thermal efficiency by using the following formula:

$$\eta_{th} = \frac{Q_u}{A_p I} \tag{6.11}$$

The performance evaluation has been carried out for fixed values of (e/D_h) and different (p/e) and 'α'.

Step.11 Thermohydraulic efficiency: Thermohydraulic performance is the performance of the system that includes the consideration of thermal as well as hydraulic characteristics is given by as;

$$\eta_{ThHyd} = \frac{Q_u - \frac{P_m}{C}}{IA_c} \tag{6.12}$$

whereas $P_m = 1.5WV^3 fL\rho$ and $C = \eta_F \eta_M \eta_{Tr} \eta_{Th}$ is the conversion factor accounting for net conversion efficiency from thermal energy of the resource to mechanical energy. By calculations the value of conversion factor comes out to be 0.2. In the conversion factor C:

η_F = Efficiency of fan or blower.

η_M = Efficiency of the electrical motor used for driving fan.

η_{Tr} = Efficiency of electrical transmission.

η_{Th} = Thermal conversion efficiency of power plant.

6.5 VALIDATION OF EXPERIMENTAL SETUP

To validate the experimental set-up, conventional flat plates were tested for which the flow and heat transfer characteristics are well known. Nu and Fr for smooth plates were computed and compared with Dittus-Boelter equation [52] and Modified Blasius equation [53] for validation. Comparison of experimental and computed value of Nu and Fr is shown by Fig. 44 and Fig. 45 respectively.

Dittus-Boelter equation: $$Nu_s = 2 \times 0.024 \,\mathrm{Re}^{0.8}\,\mathrm{Pr}^{0.4} \quad (6.13)$$

Modified Blasius equation: $$f_s = 2 \times 0.085 \,\mathrm{Re}^{-0.25} \quad (6.14)$$

For implementing the Dittus–Boelter and Modified Blasius equation for DPSAH, a constant of magnitude 2 is multiplied to the equation.

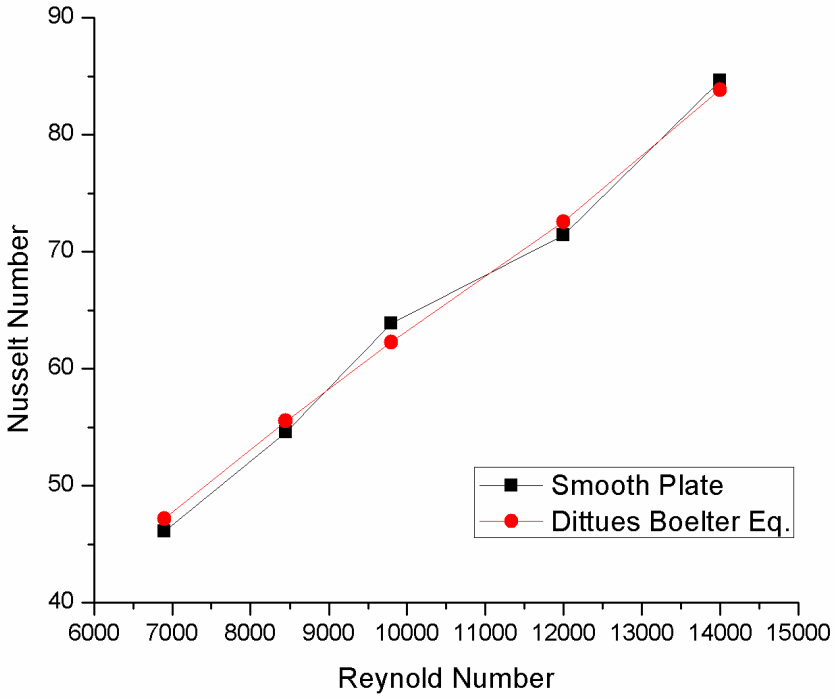

Figure 43 Nu vs Re

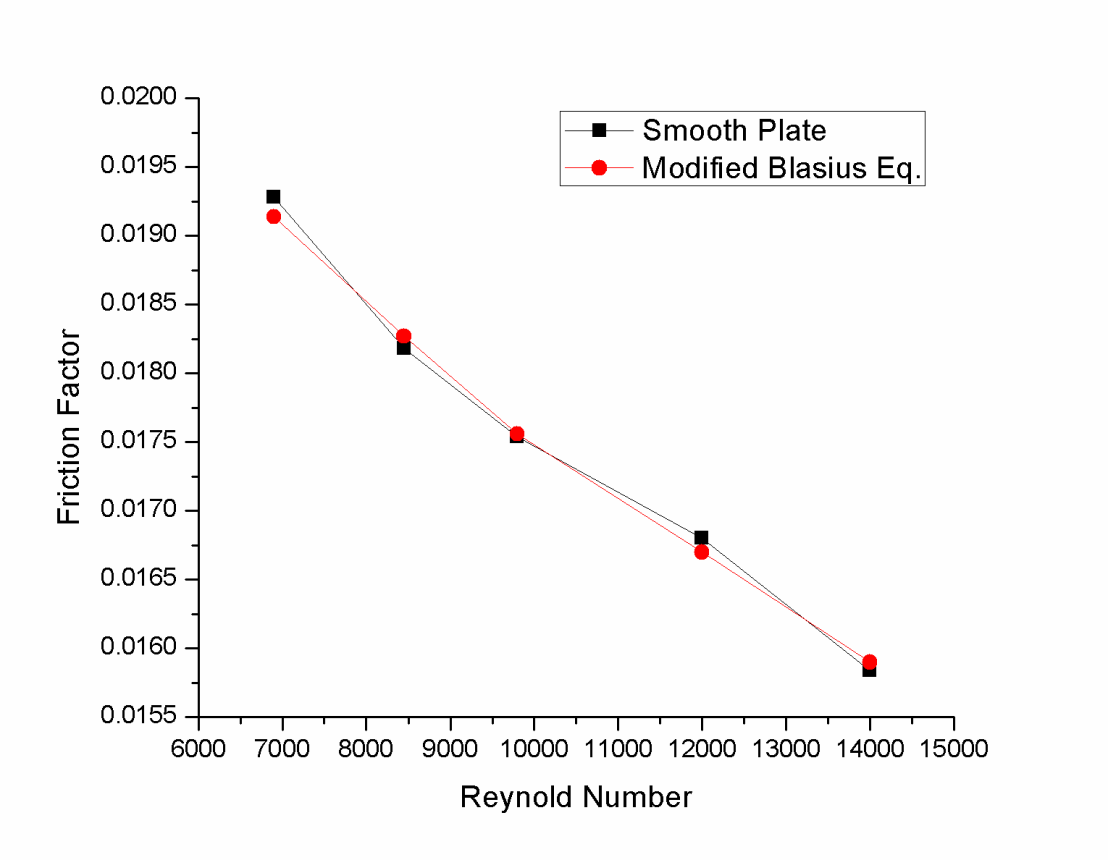

Figure 44 Fr vs Re

A deviation of 5.2% and 3.1% is observed between experimental and computed values for Nusselt number and Friction factor, which validates the experimental setup.

CHAPTER 7 RESULTS AND DISCUSSION

7.1 INTRODUCTION

To improve the heat transfer of fluid flowing in DPSAH, artificial roughness is created on both sides of the absorber surface. The objective of the present investigation is to improve the heat transfer and Fr and to improve the efficiency of DPSAH which depends upon the following roughness and operating parameter as given in Table. 2.

Table 2

S.No.	Parameters	Symbols	Ranges
1.	Reynold number	Re	6900-14000
2.	Relative roughness height	e/D_h	0.044
3.	Relative roughness pitch	p/e	5-20
4.	Aspect ratio	W/H	10
5.	Angle of attack	α	30˚-90˚

7.2 HEAT TRANSFER AND FRICTION FACTOR CHARACTERISTICS

7.2.1 Nusselt Effect

The effect of Nu verses Re, and Fr verses Re are illustrated in Fig. 46 and Fig. 47 respectively with the discrete ribs on the both side of absorber plate having a fixed value of (e/D_h) of 0.044 and (α) of 60˚ .The other parameters are p/e of 5 to 20 and Reynold number which varies from 6900 to14000. It is experimental that the Nu increases and Fr decreases with Reynold number due to suppression of laminar layer for fully developed turbulence layer in DPSAH [54]. The value of Nu and Fr are higher than smooth surface. The maximum value of Nu and Fr at (p/e) of 10 and (α) of 60˚.

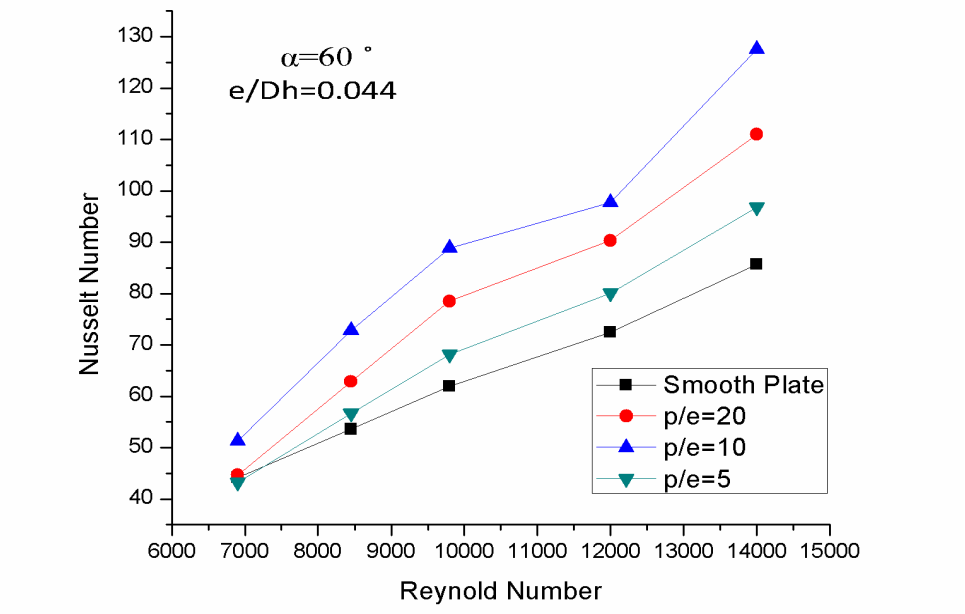

Figure 45 Nu Vs Re

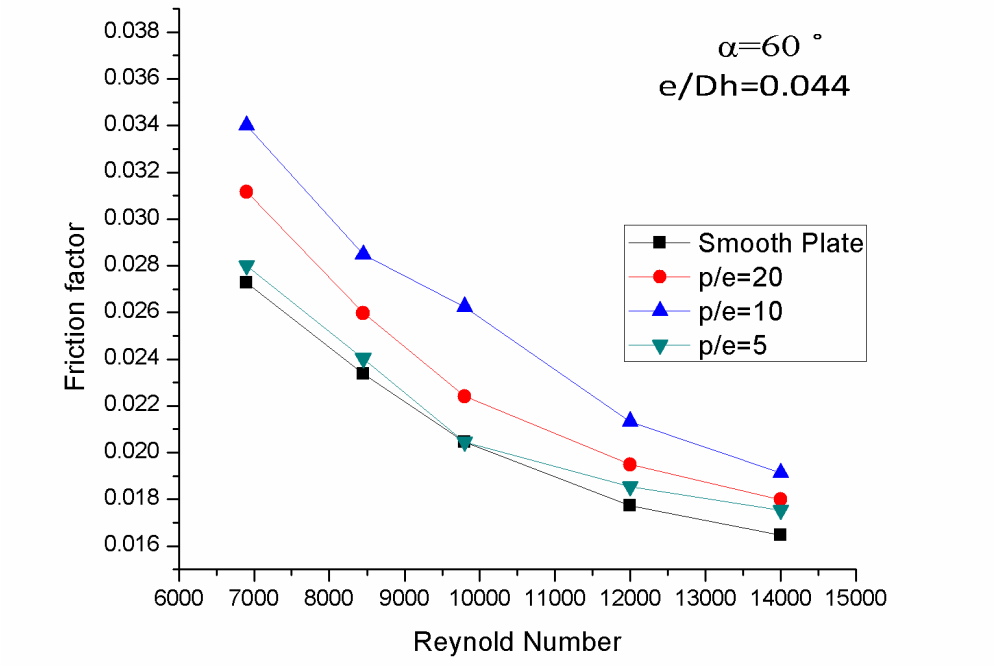

Figure 46 Fr vs Re

7.2.2 p/e Effect

Fig. 48 and Fig. 49 illustrate the effect of e/Dh on Nu, and Fr for different value of Reynold number from 6900 to14000 respectively. The graph has been plotted to compare the discrete roughness element on absorber plate for different value of (p/e) of 5, 10 and 20. The value of (α) 60° and e/Dh of 0.044. The graph shows that the Nu growths up to p/e of 10 and then decreases .It is due to the increase in the reattachment point. Also augmentation in heat transfer take place which results in the decrement in reattachment point. Fig. 49 shows that Fr

fall down with the increase in Reynold number and the maximum Fr occur at relative roughness pitch of 10.

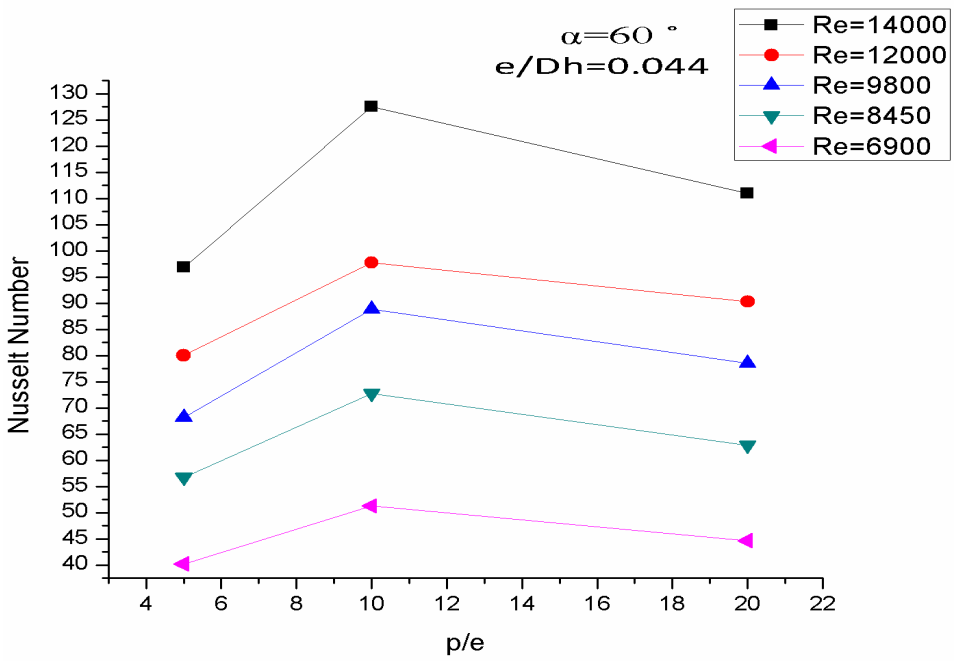

Figure 47 Nu vs (p/e)

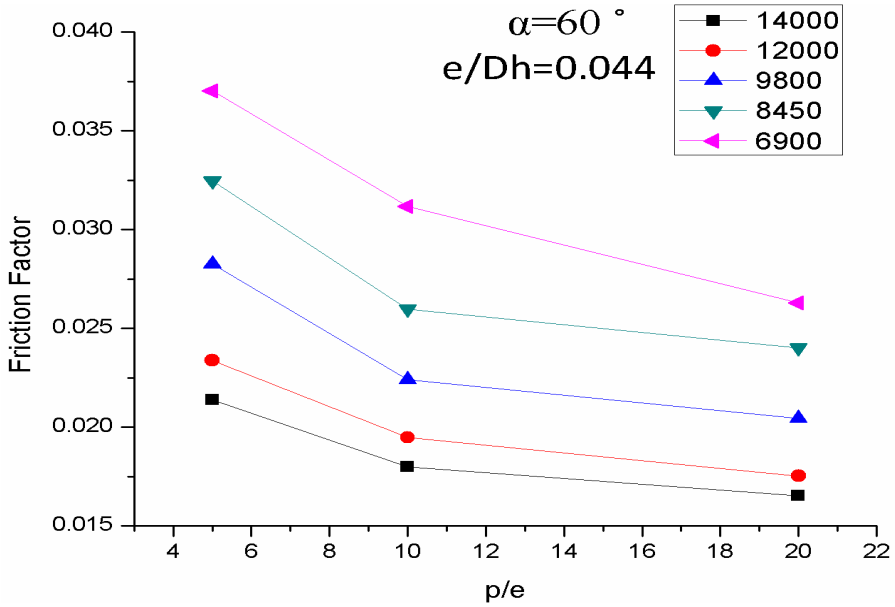

Figure 48 Fr vs (p/e)

7.2.2 Effect of Angle of Attack (α)

Fig. 50 illustrate that the Nu verses Re for angle of attack (α) of 30˚, 60˚ and 90˚; and for fixed value of (e/D_h) of 0.044 and (p/e) of 10 . Fig. 51 illustrate the effect of angle of attack (α) at 30˚, 60˚ and 90˚ on Nu for different value of Re. It is experiential that the Nu escalations

with the escalation in angle of attack because flow creates anti-rotating secondary flow [55, 56].

Fig. 52 illustrate that Fr deceases with Rey increases for different value of angle of attack (α) of 30˚, 60° and 90˚; and for fixed value of (e/D_h) of 0.044 and (p/e) of 10 .Fig. 53 illustrate that the variation of Fr with (α) for different value of Reynold number. The graph shows that anti rotating flow increases from 30° to 60˚ and then it starts decreasing from 60° to 90˚. It is obtained that the maximum friction factors occur at angle of attack (α) of 60°due to maximum anti rotating secondary flow occur at angle of attack.

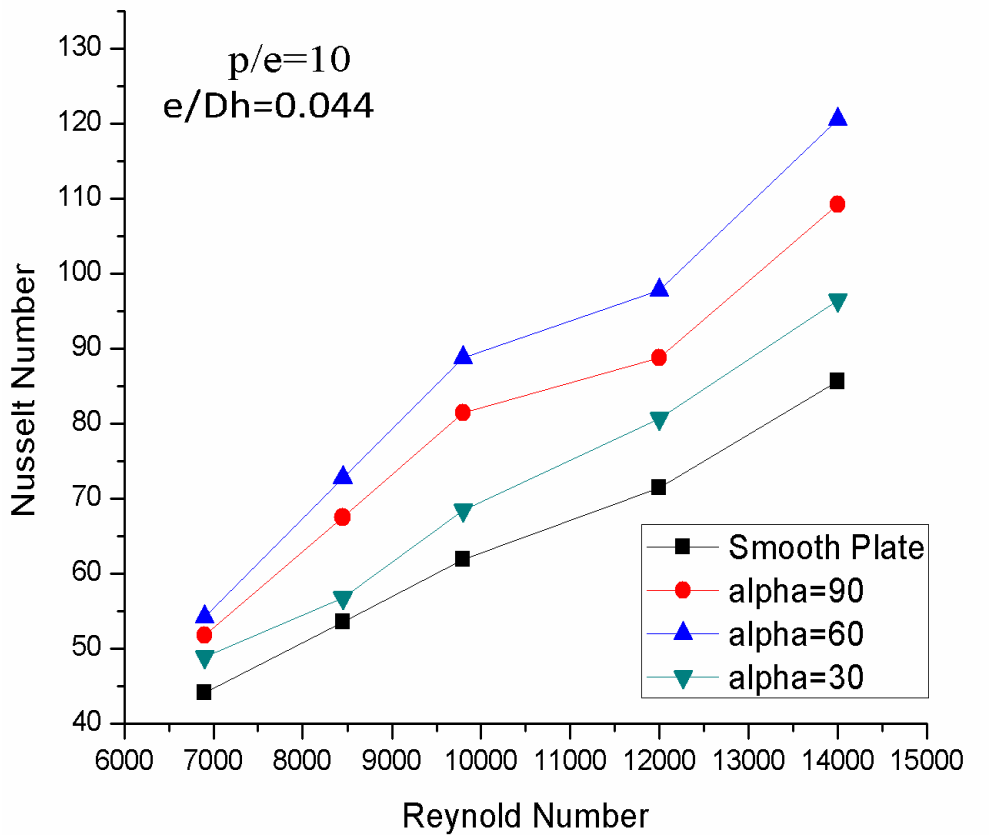

Figure 49 Nu Vs Re

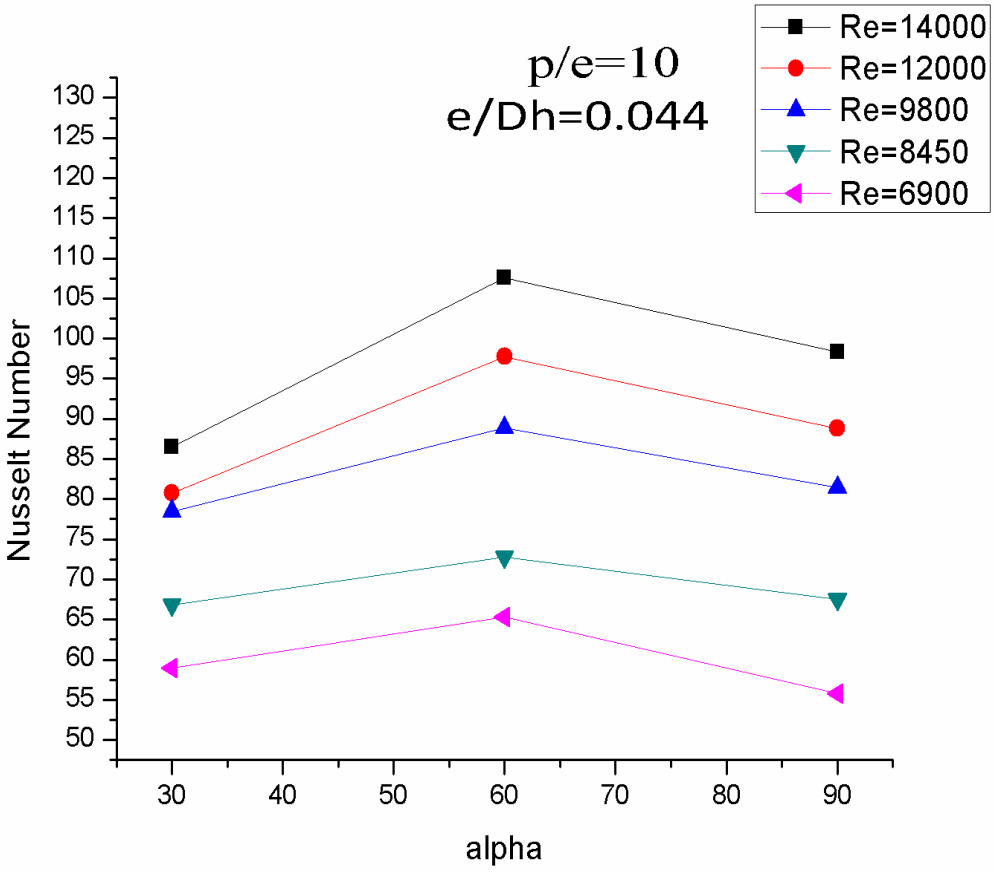

Figure 50 Nu vs alpha

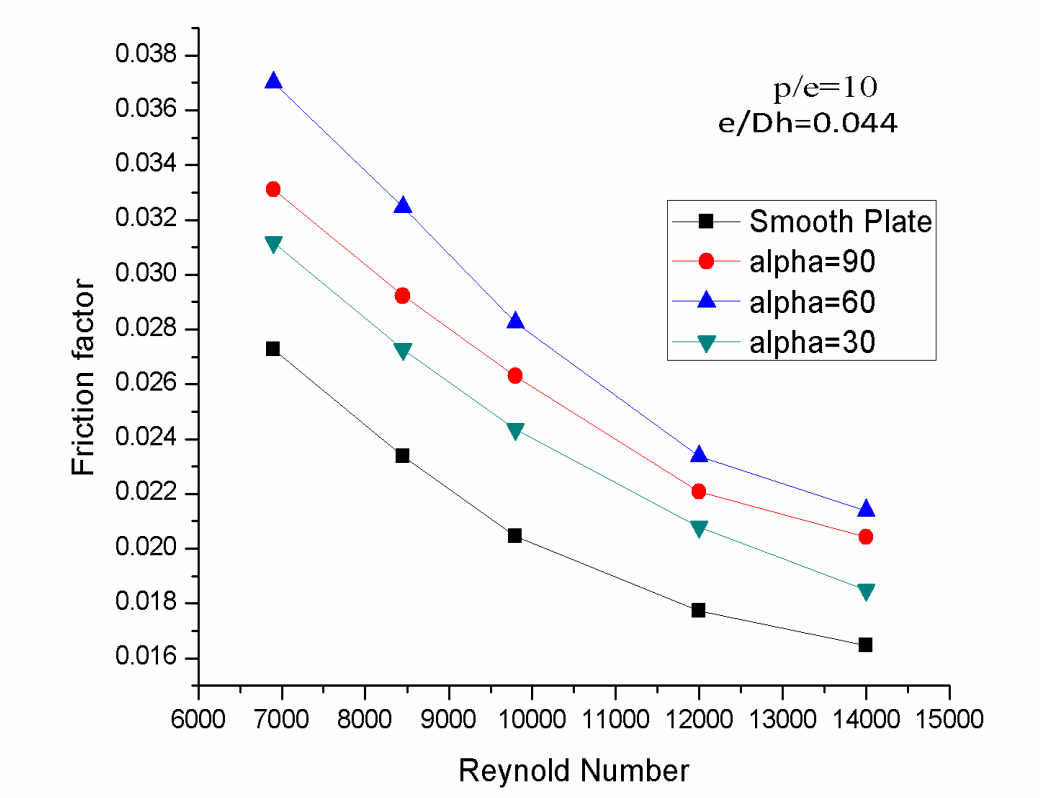

Figure 51 Fr vs Re

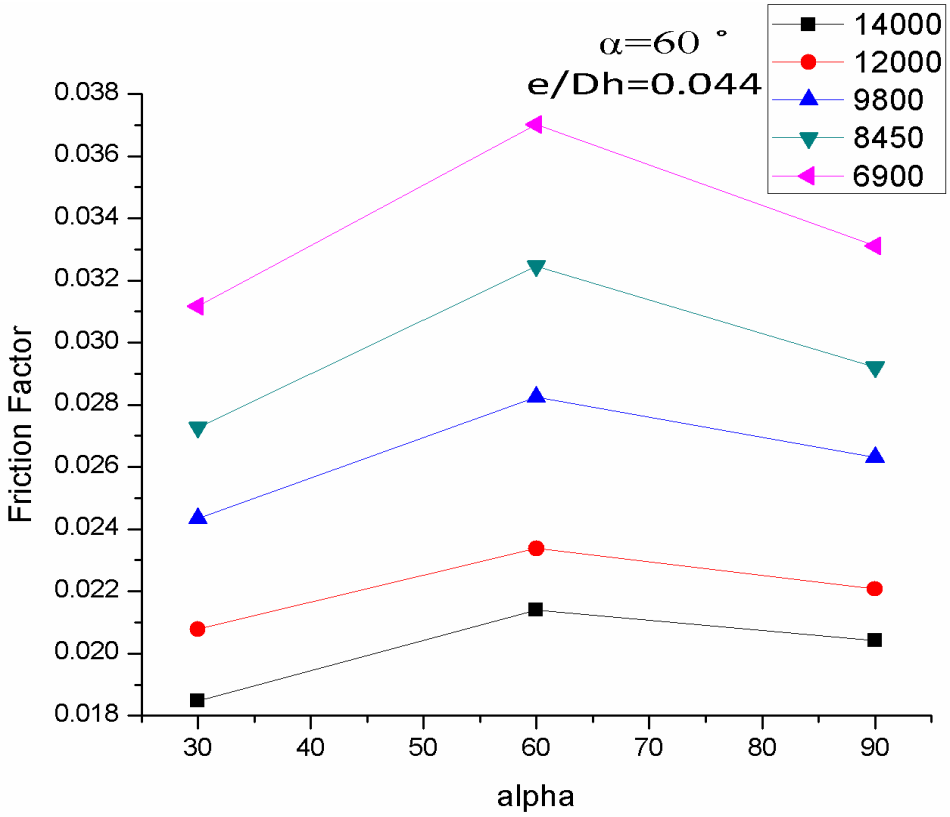

Figure 52 Fr vs Re

7.2.3 Results

The observation of from the above discussion is that the maximum Nu and Fr has been obtained 1.48 and 1.3 times respectively than the smooth plate at (p/e) of 10 and (α) of 60˚.

7.3 THERMAL EFFICIENCY

7.3.1 Effect of (p/e)

Thermal efficiency of double pass solar air heater with Re is illustrated in Fig. 54 for fixed value of (e/D_h) at 0.044 and (α) at 60°. The values of (p/e) varies from 5 - 20 and range of Reynold number varies from 6900-14000. The graph illustrate that the maximum thermal efficiency is obtained at (p/e) of 10 and it is also observed the efficiency of relative roughness pitch of 20 is more than p/e of 5. The efficiencies of roughened absorber plate are compared with the smooth plate which shows that the roughened absorber surface increases the efficiency of air heater due to the separation of flow.

7.3.2 Effect of 'α'

Thermal efficiency of DPSAH with the Reynolds number is illustrated in Fig. 55 for a fixed value of (e/D_h) at 0.044 and (p/e) at 10.The 'α' varies from 30° to 90° and range of Re is from 6900-14000. It has been observed that with the increase in'α', the thermal efficiency also increases up to 'α' of 60° after that it starts decreasing from 60° to 90°.This is due to the formation of anti-rotating secondary flow along the full length of the test section which causes length wise variation in heat transfer coefficient [55, 56]. The maximum thermal efficiency is obtained at 'α' of 60°. After that the anti-rotating secondary flow starts decreasing and due to this efficiency decreases which lowers the thermal efficiency for an angle of 90° than 60^o. Moreover the efficiency of 90° is higher than that of 30° because anti-rotating secondary flow is more prominent at the later section of the angle.

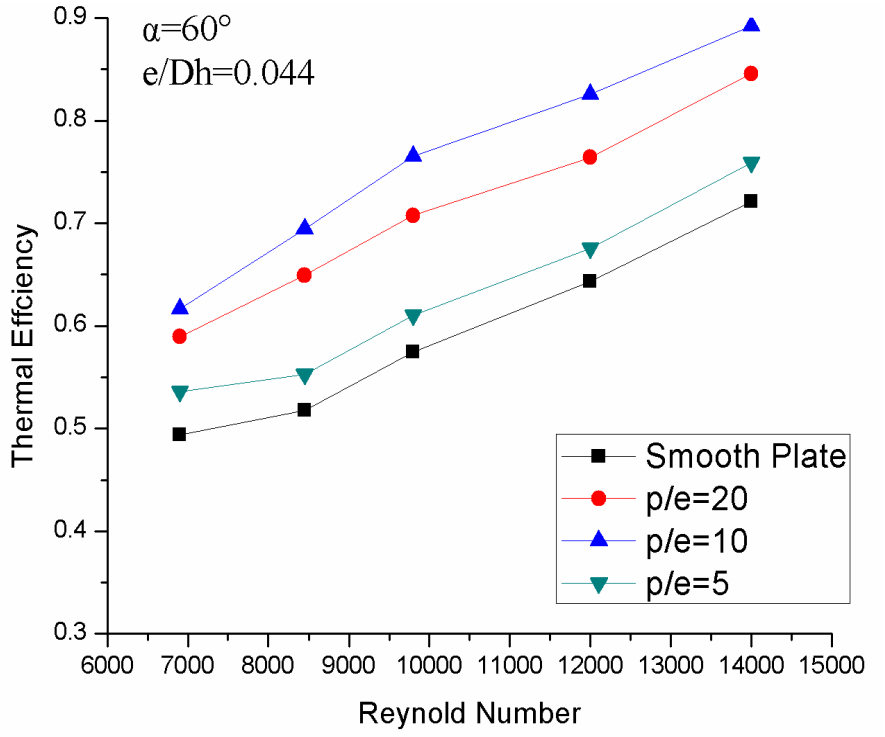

Figure 53 Thermal Efficiency vs Re

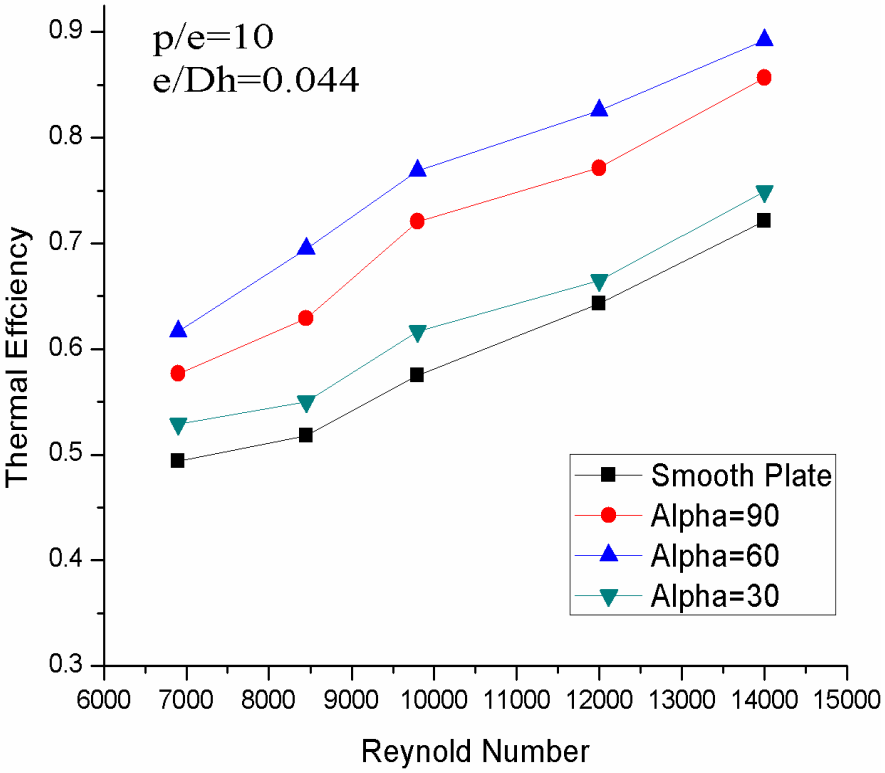

Figure 54 Thermal Efficiency vs Re

7.3.3 Results

The observation of Fig. 54 and Fig. 55 shows that the maximum thermal efficiency of double pass solar air heater at (p/e) of 10 and 'α' of 60° is 89.25% and enhancement of thermal efficiency of roughened absorber plate is 23.71% higher than the smooth plate.

7.4 THERMOHYDRAULIC EFFICIENCY

The thermohydraulic performance in terms of an effective efficiency of the solar energy collection system is determined on the basis of actual thermal gain, to generate power needed for pumping air through the collection system. The effective efficiency of roughened as well as smooth absorber plate solar air heater has been computed on the basis of the method proposed by Cortes and Piacentini [57].

7.4.1 Effect of 'p/e'

Thermohydraulic efficiency of DPSAH with Re is shown in Fig. 56 for fixed value of (e/D_h) at 0.044 and 'α' at 60°.

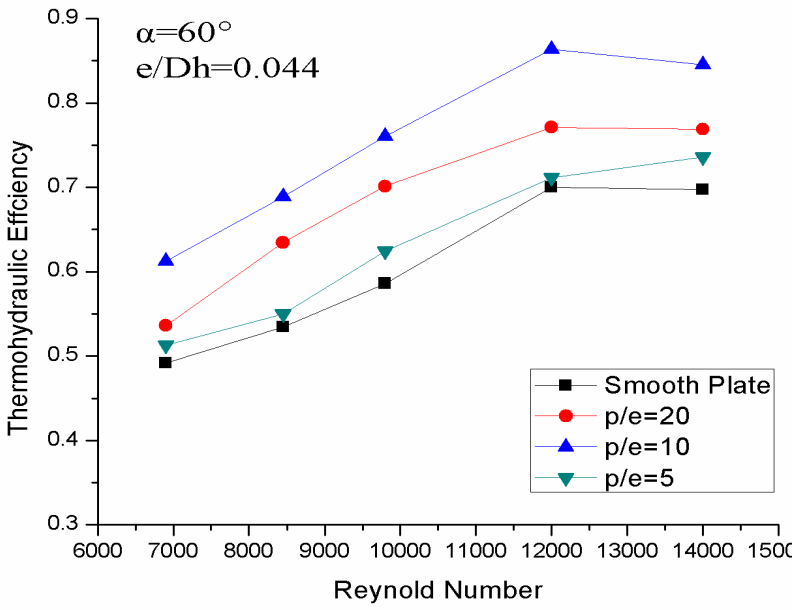

Figure 55 Thermohydraulic Efficiency vs Re

7.4.2 Effect of Angle of Attack (α)

Thermohydraulic efficiency of DPSAH with the Re is illustrated in Fig. 57 for fixed value of (e/D_h) at 0.044 and (p/e) at 10.The 'α'varies from 30° to 90° and range of Reynold number varies from 6900-14000. It has been experiential that with the increase in 'α', the

thermohydraulic efficiency also increases up to the 'α' of 60° after that it starts decreasing or near to equivalent from 60° to 90°.

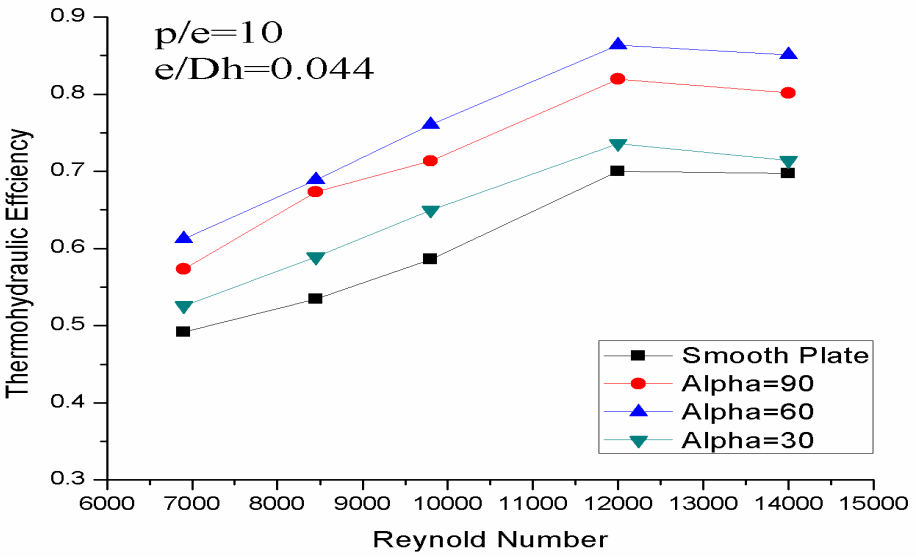

Figure 56 Thermohydraulic Efficiency vs of Re

7.4.3 Results

The observation of Fig. 56 and Fig. 57 shows that the maximum thermohydraulic efficiency of double pass solar air heater at relative roughness pitch (p/e) of 10 and angle of attack of 60° is 86.31% and enhancement of thermohydraulic efficiency of roughness absorber plate is 24.2% higher than the smooth plate.

7.5 CORRELATIONS

The correlations have been developed for DPSAH having ribs on both sides of the absorber surface which results in higher heat transfer rate and Fr characteristics. The ranges of operating parameter are given below in the Table. 2. The functional relationship for Nu and Fr as 'f'can be written as:

$$Nu = Nu\left(\mathrm{Re}, p/e, \alpha, e/D_h\right) \tag{7.1}$$

$$f = f\left(\mathrm{Re}, p/e, \alpha, e/D_h\right) \tag{7.2}$$

7.5.1 Correlation for Nusselt Number

The Nu verses Re is illustrated in Fig. 58. It shows that the Nu and Re have almost relationship of linear. The straight line equation is represented as;

$$Nu = A_0\,\mathrm{Re}^{1.0869} \tag{7.3}$$

The coefficient of A_0 will in fact be a function of another influencing parameter as relative roughness height, angle of attack and relative roughness parameter. The value of the coefficient A_0 = 3.1×10-3.Now taking the parameter angle of attack (α/60°) and plot the graph between (Nu/Re1.0869) and (α/60°) on natural log scale shown in Fig. 59.

A regression analysis is implemented to fit a second order polynomial is expressed by;

$$\ln\left(\frac{Nu}{\mathrm{Re}^{1.0869}}\right) = B_0 + B_1 \ln(\alpha/60) + B_2 \ln(\alpha/60)^2 \qquad 7.4$$

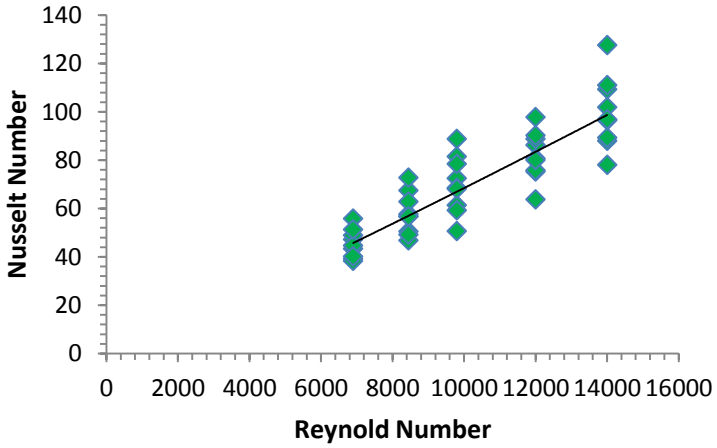

Figure 57 Plot of Nu vs Re

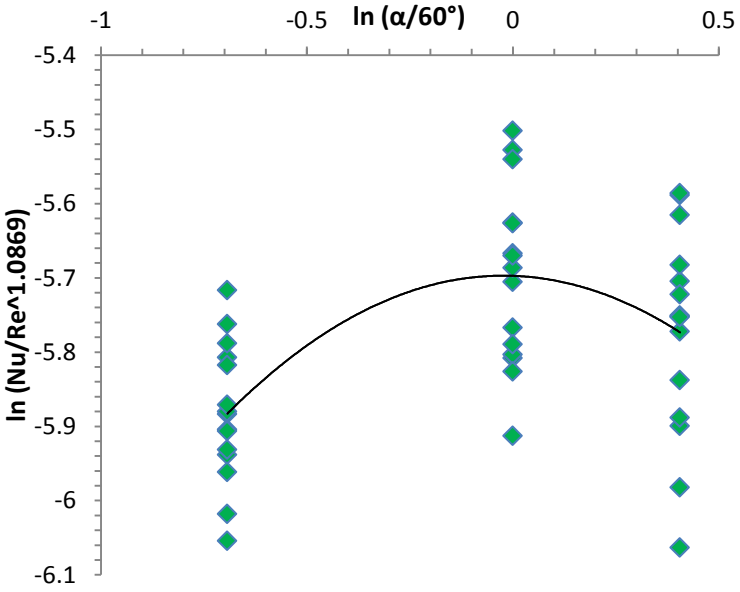

Figure 58 Plot of ln(Nu/Re^1.0869) vs ln(α/60°)

This equation can be expressed as:

$$\frac{Nu}{\mathrm{Re}^{1.0869}} = B_0(\alpha/60)^{-0.195}\exp\left[-0.4143(\ln(\alpha/60))^2\right] \quad 7.5$$

The value of the coefficient B_0 = -5.69739. The value B_0 of has been plotted against relative roughness pitch (p/e) is shown in Fig.60.

$$\frac{Nu}{\mathrm{Re}^{1.0869}(\alpha/60)^{-0.195}\exp\left[-0.4143(\ln(\alpha/60))^2\right]} = B_0 \quad 7.6$$

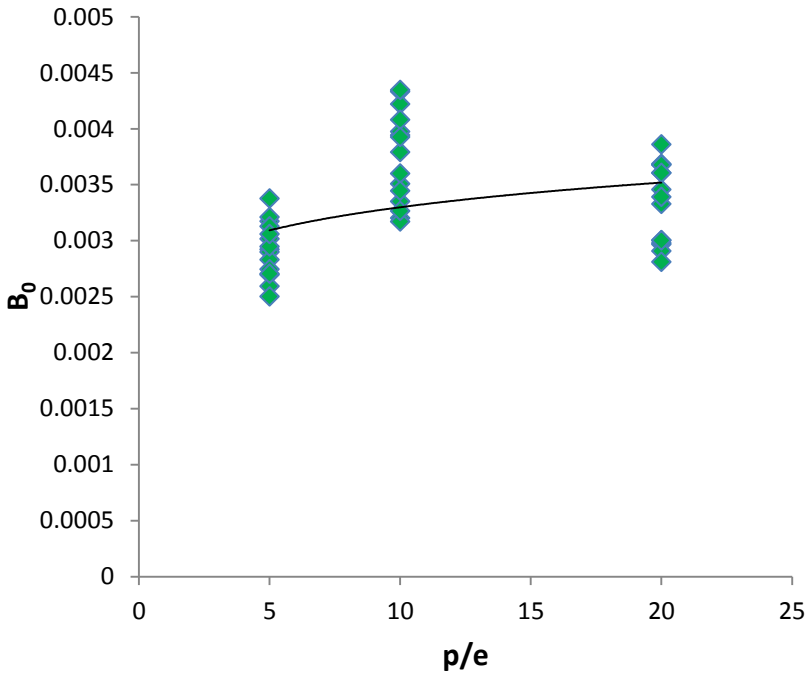

Figure 59 Plot of B_0 vs p/e

From Fig. 60 the expressed equation as given below

$$\frac{Nu}{\mathrm{Re}^{1.0869}(\alpha/60)^{-0.195}\exp\left[-0.4143(\ln(\alpha/60))^2\right]} = C_0(p/e)^{0.0933} \quad 7.7$$

The value of the coefficient $C_0 = 2.7\times10^{-3.}$

Nu correlation is obtained from the different operating parameters are given below:

$$Nu = 2.7\times10^{-3}\times\mathrm{Re}^{1.0869}\times(\alpha/60)^{-0.195}\times\exp\left[-0.4143(\ln(\alpha/60))^2\right]\times(p/e)^{0.0933} \quad 7.8$$

7.5.2 Correlation for Fr

The Fr verses Re is illustrated in Fig. 61. It shows that the friction factor and Reynold number have almost linear relationship. The straight line equation is represented as;

$$f = D_0 \, \mathrm{Re}^{-0.642} \tag{7.9}$$

The value of the coefficient $D_0 = 0.5737$.

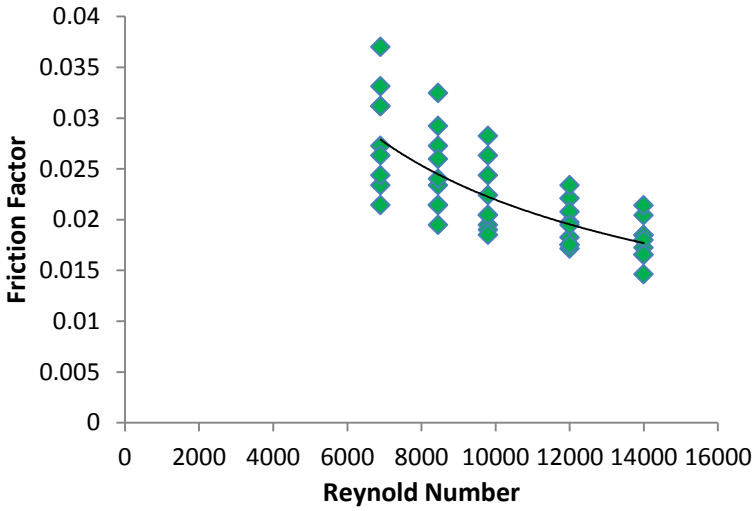

Figure 60 Plot of Fr vs Re

Now taking the parameter (α/60°) and plot the graph between (*f*/Re^1.0869) and (α/60°) on natural log scale shown in Fig. 62 and equation express as given below

$$\ln\left(\frac{f}{\mathrm{Re}^{-0.642}}\right) = E_0 + E_1 \ln(\alpha/60) + E_2 \ln(\alpha/60)^2 \tag{7.10}$$

This equation can be expressed as:

$$\frac{f}{\mathrm{Re}^{-0.642}} = E_0 (\alpha/60)^{-0.0128} \exp\left[-0.3257(\ln(\alpha/60))^2\right] \tag{7.11}$$

The value of the coefficient $E_0 = -5.69739$.

Now considering the parameter (p/e), the value E_0 of has been plotted against (p/e) is shown in Fig. 63.

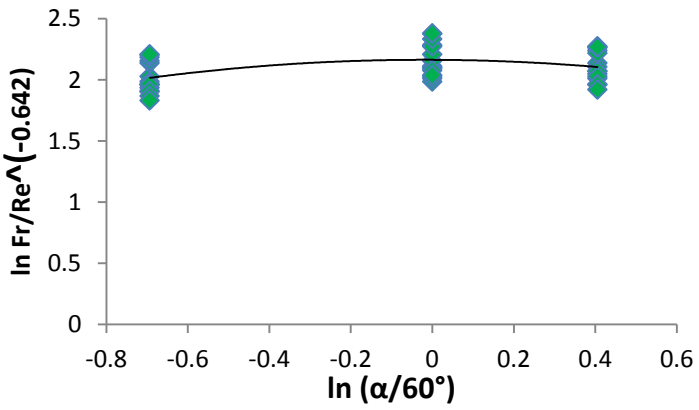

Figure 61 Plot of ln (Fr/Re^(-0.642)) vs ln (α/60°)

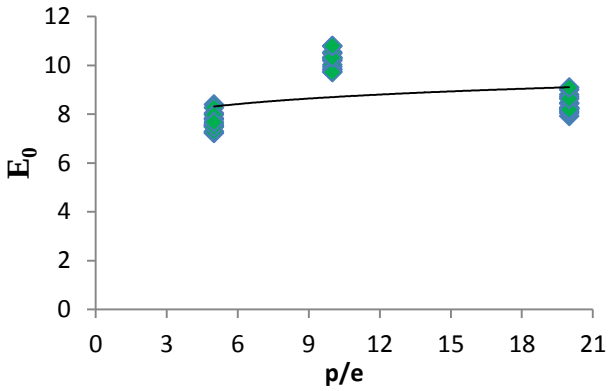

Figure 62 Plot E_0 vs p/e

$$\frac{Nu}{\mathrm{Re}^{-0.642}(\alpha/60)^{-0.0128}\exp\left[-0.3257(\ln(\alpha/60))^2\right]} = E_0 \qquad 7.12$$

The equation expressed as given below:

$$\frac{Nu}{\mathrm{Re}^{-0.642}(\alpha/60)^{-0.0128}\exp\left[-0.3257(\ln(\alpha/60))^2\right]} = F_0(p/e)^{7.4813} \qquad 7.13$$

The value of the coefficient $C_0 = 2.7\times10^{-3.}$

The correlations Fr is given below as;

$$f = 7.4813\times\mathrm{Re}^{-0.642}\times(\alpha/60)^{-0.0128}\times\exp\left[-0.3257(\ln(\alpha/60))^2\right]\times(p/e)^{-0.309} \qquad 7.14$$

7.5.3 Results

The evaluation of the experimental and computed values of the Nu and Fr are given in Fig. 64 and Fig. 65 respectively. Fig. 64 shows the deviation of ±10.53% between the experimental and computed values of the Nusselt number which is in a fair acceptable limit. Fig. 65 shows the deviation of ±9.67% between the experimental and computed values of friction factor which is also in good acceptable limit.

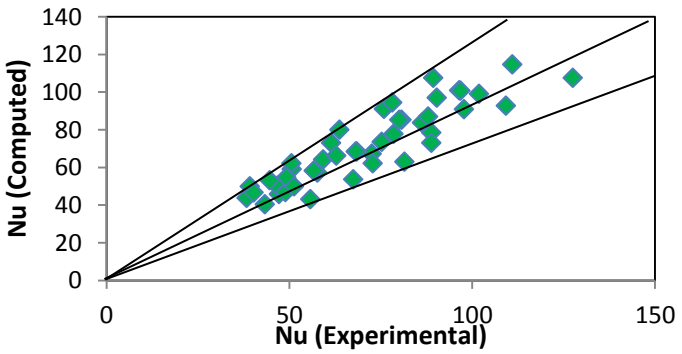

Figure 63 Computed and experimental values of Nusselt Number

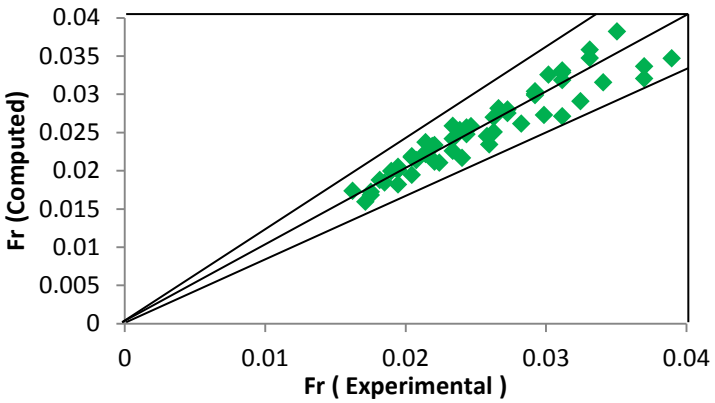

Figure 64 Computed and experimental values of Friction Factor

CHAPTER 8 CONCLUSION AND FUTURE SCOPE

An experimental investigation has been performed in DPSAH which having roughened element on both sides of the absorber plate. The effect of p/e, e/Dh and angle of attack (α) on the Nu and Fr have been analyzed to increase the enactment of DPSAH. The major conclusions and future scope are highlighted below:

8.1 CONCLUSIONS

The maximum heat transfer and Fr attains maximum value at (p/e) of 10 and (α) of 60° for the fixed value of (e/D_h) of 0.044. The enhancements of the Nu and Fr have been obtained 1.48 & 1.3 times respectively against the smooth plate. The correlations for the Nu and Fr have been derivative as a function of Re, p/e and (α). The maximum deviation of investigational value and computed value of Nu from the correlation is found to be ±10.53%. Also maximum deviation of experimental value and computed value of Fr from the correlation is found to be ±9.67%.The maximum values of thermal and thermohydraulic efficiency occur at (p/e) of 10 and (α) of 60° at (e/Dh) of 0.044 is constant.

8.2 FUTURE SCOPE

The major applications of DPSAH are establish to be in space heating, gymnasiums, dryers, food dehydration etc. This DPSAH is better than the SPSAH in context that it is having better efficiency than the later one. Also we can simulate the experimental results in CFD and mathematical modeling so to get the better results and to use it in best possible way.

REFERENCES

[1] Raja AK, Srivatava Amit P, Dewivedi Manish.Power Plant Engineering. New Delhi: New Age International Publishers;

[2] Rai GD. Non-Conventional energy sources. New Delhi: Khanna Publication;1997

[3]Sukatme SP. Solar energy principle collection and storage. 2nd ed. New Delhi:Tata McGraw-Hill; 2006

[4] Kalogeriou, Soteris. Recent Patents in Solar Energy Collectors and Applications Recent. Patents on Engineering 2007; 1: 23-33

[5] Duffie, Beckman. Solar engineering of thermal processes. 2nd ed. New York: A Wiley International Science Publication;1980

[6] Kalogirou, Soteris. Solar Thermal Collectors and Applications. Progress in Energy and Combustion Science 2004; 30: 231-95.

[7] Dan Arvizu, Palani Balya. Direct Solar Energy, Renewable energy sources and Climate change Mitigation. New York:Cambridge University Press; 2012

[8] Patil AK, Saini JS, Kumar K. A comprehensive review on roughness geometries and investigation techniques used in artificially roughened solar air heaters. International Journal of Renewable Energy Research 2012; 2(1):1-15

[9] Garg HP and Prakash, JP. Solar Energy- Fundamentals and Applications. New Delhi:Tata McGraw-Hill; 2006

[10] Parwar CB, Aharwal KR, Chaube Alok. Heat transfer and fluid flow characteristics of rib-groove roughened solar air heater ducts. Indian Journal of Science and Technology 2009; 2(11):50-54

[11] Thakur SK, Kumar NS, Kumar Anoop, Mittal Vijay. Use of artificial roughness to enhance heat transfer in solar air heaters a review. Journal of Energy in Southern Africa 2010; 21(1):35-51

[12] Shakya Uttara, Saini RP, Singhal MK. A review on artificial roughness geometry for enhancement of heat transfer and friction characteristics on roughened duct of solar air heater. International Journal of Emerging Technology and advanced Engineering 2013; 3(6): 279-287

[13] Gawande VB, Dhoble AS, ZOdpe DB. Effect of roughness geometries on heat transfer enhancement in solar thermal system- A review. Renewable and Sustainable Energy Reviews 2014; 32:347-378

[14] Prasad BN, Saini JS. Effect of artificial aoughness on heat transfer and friction factor in a solar air heater. Solar Energy 1988; 41(6):555-560

[15] Gupta D, Solanki SC, Saini JS. Thermohydraulic performance of solar air heater with roughened absorber plates. Solar energy 1997; 61:33-42

[16] Varshney L , Saini JS. Heat transfer and friction factor correlations for rectangular solar air heater duct packed with wire mesh screen matrices. Solar Energy 1998; 62(4):255-262

[17] Ebrahim-Momin Abdul-Malik, Saini JS, Solanki SC. Heat transfer and friction in solar air heater duct with V-shaped rib roughness on absorber plate. International Journal of Heat and Mass Transfer 2002; 45:3383–3396

[18] Bhagoria JL, Saini JS, Solanki SC. Heat transfer coefficient and friction factor correlation for rectangular solar air heater duct having transverse wedge shape rib roughness on the absorber plate. Renewable Energy 2002; 25:341-369

[19] Togrul IT, Pehliven Dursun, Akosman Cevdet. Development and testing of solar air heater with conical concentrator. Renewable Energy 2004; 29:263–275

[20] Sahu MM, Bhagoria JL. Augmentation of heat transfer coefficient by using 90° broken transverse ribs on absorber plate of solar air heater, Renewable Energy 2005; 30:2057-2063

[21] Jaurker AR, Saini JS, Gandhi BK. Heat transfer and friction characteristics of rectangular solar air heater duct using rib-grooved artificial roughness. Solar Energy 2006; 80:895–907

[22] Varun, Saini RP, Singal SK. Investigation of thermal performance of solar air heater having roughness elements as a combination of inclined and transverse ribs on absorber plate. Renewable energy 2008; 133:1398-1405

[23] Aharwal KR, Gandhi BK, Saini JS. Heat transfer and friction characteristics of solar air heater ducts having integral inclined discrete ribs on absorber plate. International Journal of Heat and Mass Transfer 2009; 52:5970-5977

[24] Prasad SB, Saini JS, Singh KM. Investigation of heat transfer and friction characteristics of packed bed solar air heater using wire mesh as packing material. Solar Energy 2009; 83:773-783

[25] Singh Sukhmeet, Chander Subhash, Saini JS. Heat transfer and friction factor correlations of solar air heater ducts artificially roughened with discrete V-down ribs. Energy 2011;36:5053-5064

[26] Bhushan Brij, Singh Ranjit. Nusselt number and friction factor correlations for solar air heater duct having artificially roughened absorber plate. Solar energy 2011; 85:1109-1118

[27] Satcunanathan S, Deonarine S. A two pass solar air heater. Solar Energy 1973; 15:141-49

[28] Wijeysundera NE, Le AH, Tjioe LE. Thermal performance study of two-pass solar air heaters. Solar Energy 1982; 28: 363–70

[29] Bansal NK, Sodha MS, Singh D. Analysis of a non-porous double-flow solar air heater. Applied Energy 1982; 12:251-258

[30] Mohamad AA. High efficiency solar air heater. Solar Energy 1997; 60(2):71-76

[31] Sopian K, Supranto, Daud WRW, Othman MY, Yatim B. Thermal performance of the double pass solar collector with without porous media. Renewable Energy 1999; 18:557-564

[32] Yeh HM, Ho CD, Hou JZ. Collector efficiency of double pass solar air heater. Energy 2002; 27: 715–727

[33] Jain Dilip, Jain RK. Performance ecaluation of an inclined multi-pass solar air heater with in-built thermal storage on deep- bed drying application. Journal of Food Engineering 2004; 65:497-509

[34] Naphon Paisarn. Effect of porous media on the performance of the double-pass flat solar air heater. International Communication in heat and mass transfer 2005; 32:140-150

[35] Naphon Paisarn. On the performance and entropy generation of the double-pass solar air heater with longitudinal fins. Renewable energy 2005; 30:1345-1357

[36] El-Sebaii AA, Ramadan MRI, Aboul-Enein S, El-Bialy E. Thermal performance of a packed bed double-pass solar air heater. Energy 2007; 32:1524-1535

[37] Esen Hikmet. Experimental energy and exergy analysis of a double –flow solar air heater having different obstacles on absorber plates. Building and environment 2008; 43: 1046-1054

[38] Esen Hikmet, Ozgen Filiz, Esen Mehmet, Sengur Abdulkadir. Modelling of a new solar air heater through least-squares support vector machines. Expert System with Application 2009; 36:10682-10682

[39] Aldabbagh LBY, Omojaro AP. Experimental performance of single and double pass solar air heater with fins and steel wire mesh as absorber. Applied Energy 2010; 87:3759-3765

[40] El-khawajah MF, Aldabbagh LBY, Egelioglu F. The effect of using wire mesh as an absorber. Solar Energy 2011; 85:1479-1487

[41] Chamoli Sunil, Chauhan Ranchan, Thakur NS, Saini, JS. A review of the performance of double pass solar air heater. Renwable and sustainable energy review 2011

[42] Kumar Rakesh, Rosen MA. Performance evaluation of a double pass PV/T solar air heater with and without fins. Applied Thermal Engineering 2011; 31:1402-1410

[43] Dhiman Prashant, Thakur NS, Kumar Anoop, Singh Satyender. An analytical model to predict the thermal performance of a novel paralle flow packed bed dolar air heater. Applied energy 2011; 88: 2157-2167

[44] Ho Chii-Dong, Yeh Ho-Ming, Chen Tsung-Ching. Collector efficiency of upward-type double-pass solar air heaters with fins attached, International Communications in heat and mass transfer 2011; 38:49-56

[45] Shalaby SM, El-Sebaii AA, Aboul-Enein S, Ramadan MRI , Moharram BM. Investigation of thermal performance of double pass-flat and v-corrugated plate solar air heaters. Energy 2011; 36:1076-1086.

[46] Shalaby SM, El-Sebaii AA, Aboul-Enein S, Ramadan MRI , Moharram BM. Thermal performance investigation of double pass- finned plate solar air heater. Applied Energy 2011; 88:1727-1739

[47] Dogra Sudhanshu. Effect of artificial roughness on heat transfer and friction factor characteristics in rectangular duct of a double pass solar air heater. International Journal of Mechanical engineering and Technology 2013; 4(3):289-298

[48] Singh Satyender, Dhiman Prashant. Recyclic double pass packed bed solar air heater. International Journal of Thermal Sciences 2015; 87:215-227

[49] Bansal NK. Solar air heater application in India. Renewable Energy 1999; 16: 618-623

[51] ASHARAE Standard 93–77. Method of testing to determine the thermal performance of Solar Air Heater, New York 1997; 1–34

[52] Bhatti, MS, Shah, RK. Turbulent and transition flow convective heat transfer. In: Kakac S, Shah RK, Aung W, editors. Handbook of Single-phase Convective Heat Transfer. New York: John Wiley andSons, 1987.

[53] Kays,W.M., Perkin H. Forced convection internal flow in ducts. In: Rohsenow W.M., Hartnett I.V,editors, Handbook of Heat Transfer. New York:McGraw-Hill.

[54] Varun, Yadav S, Kaushal Maneesh, Siddhartha. Nusselt number and friction factor correlations for solar air heater duct having prptrusions as roughness elements on absorber plate. Experimental Thermal and Fluid Science 2013; 44:34-41

[55] Hans VS, Saini RP and Saini JS. Performance of artificially roughened solar air heaters – A review. Renewable and Sustainable Energy Reviews 2010; 13:1854-1869.

[56] Singal SK, Saini RP, Varun. A review on roughness geometry used in solar air heaters. Solar Energy 2007; 81:1340-1350

[57] Cortes A, Piacentini R. Improvement of the efficiency of a bare solar collector by means of turbulent promoters, Applied Energy 1990; 36:253-261